Science of the Total Environment 869 (2023) 161688

Contents lists available at ScienceDirect

Science of the Total Environment

journal homepage: www.elsevier.com/locate/scitotenv

Comparative assessment of energy generation from ammonia oxidation by different functional bacterial communities ☆

Vitor Cano [a,b,*], Marcelo A. Nolasco [a], Halil Kurt [b,1], Chenghua Long [b], Julio Cano [a], Sabrina C. Nunes [a], Kartik Chandran [b]

[a] University of São Paulo, School of Arts, Sciences and Humanities, Av. Arlindo Béttio, 1000, Sao Paulo, SP 03828-000, Brazil
[b] Columbia University, Department of Earth and Environmental Engineering, 500 West 120th Street, Room 1045 Mudd Hall, New York, NY 10027, United States

HIGHLIGHTS

- Electrogen, AOB and anammox biofilms achieved different power levels in MFCs.
- Electrogen rich biofilm adapted to oxidize ammonia and yielded highest power.
- Nitrite accumulation was observed without known nitrifying bacteria presence.
- O_2 and SO_4^{2-} are limiting factors for current generation by AOB.
- N-NH_4^+ oxidation by anodophilic bacteria was combined with cathodophilic activity.

GRAPHICAL ABSTRACT

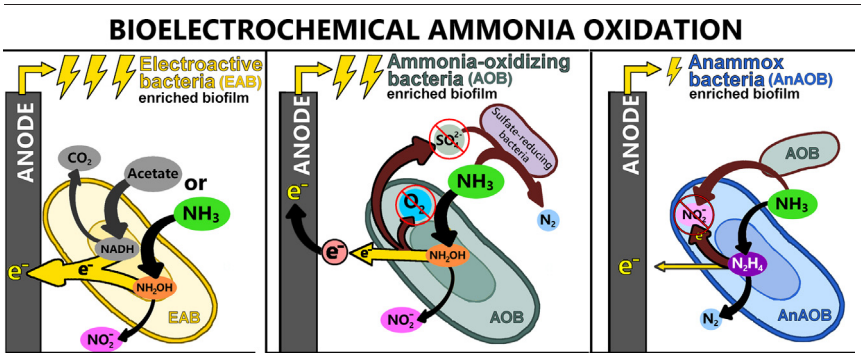

ARTICLE INFO

Editor: Yifeng Zhang

Keywords:
Bioelectrochemical system
Circular economy
Waste-to-energy
Anodophilic nitrification
Wastewater treatment plant
Green technologies

ABSTRACT

Bioelectrochemical ammonia oxidation (BEAO) in a microbial fuel cell (MFC) is a recently discovered process that has the potential to reduce energy consumption in wastewater treatment. However, level of energy and limiting factors of this process in different microbial groups are not fully understood. This study comparatively investigated the BEAO in wastewater treatment by MFCs enriched with different functional groups of bacteria (confirmed by 16S rRNA gene sequencing): electroactive bacteria (EAB), ammonia oxidizing bacteria (AOB), and anammox bacteria (AnAOB). Ammonia oxidation rates of 0.066, 0.083 and 0.082 g NH_4^+-N L^{-1} d^{-1} were achieved by biofilms enriched with EAB, AOB, and AnAOB, respectively. With influent 444 ± 65 mg NH_4^+-N d^{-1}, nitrite accumulation between 84 and 105 mg N d^{-1} was observed independently of the biofilm type. The AnAOB-enriched biofilm released electrons at higher potential energy levels (anode potential of 0.253 V vs. SHE) but had high internal resistance (R_{int}) of 299 Ω, which limits its power density (0.2 W m^{-3}). For AnAOB enriched biofilm, accumulation of nitrite was a limiting factor for power output by allowing conventional anammox activity without current generation. AOB enriched biofilm had R_{int} of 18 ± 1 Ω and yielded power density of up to 1.4 W m^{-3}. The activity of the AOB-enriched biofilm was not dependent on the

Abbreviations: AMO, ammonia monooxygenase; AOB, ammonia-oxidizing bacteria; AQDS, 9,10-anthraquinone-2,6-disulfonic acid; BEAO, bioelectrochemical ammonia-oxidation; BES, bioelectrochemical systems; AnAOB, anaerobic ammonia-oxidizing bacteria; CEM, cation exchange membrane; COD, chemical oxygen demand; CE, coulombic efficiency; DO, dissolved oxygen; EAB, electroactive bacteria; EET, extracellular electron transfer; EPS, extracellular polymeric substances; GAC, granular activated carbon; Hdh, hydrazine dehydrogenase; HAO, hydroxylamine oxidoreductase; MEC, microbial electrolysis cell; MFC, microbial fuel cell; NOB, nitrite-oxidizing bacteria; NXR, nitrite oxidoreductase; OCP, open-circuit potential; SRM, sulfate-reducing microorganisms; SM, supplementary material; WWTP, wastewater treatment plant.

☆ Statements relating to our ethics and integrity policies: Data utilized in the study is available in the supplementary information or publicly available at NCBI (BioProject ID: PRJNA803873). The authors declare that they have no known competing financial interests or personal relationships that could have appeared to influence the work reported in this paper, which is in compliance with the Ethics in Publishing Policy.

* Corresponding author at: University of São Paulo, School of Arts, Sciences and Humanities, Av. Arlindo Béttio, 1000, Sao Paulo, SP 03828-000, Brazil.
E-mail addresses: vitorc@usp.br (V. Cano), mnolasco@usp.br (M.A. Nolasco), halil.kurt@sbu.edu.tr (H. Kurt), cl3402@columbia.edu (C. Long), julio.cano@usp.br (J. Cano), sc.nunes@usp.br (S.C. Nunes), kc2288@columbia.edu (K. Chandran).
[1] Present address: University of Health Sciences, Hamidiye International Faculty of Medicine, Department of Medical Biology, Istanbul, Turkey.

http://dx.doi.org/10.1016/j.scitotenv.2023.161688
Received 27 September 2022; Received in revised form 13 January 2023; Accepted 14 January 2023
Available online 25 January 2023

accumulation of dissolved oxygen and achieved 1.5 fold higher coulombic efficiency when sulfate was not available. The EAB-enriched biofilm adapted to oxidize ammonia without organic carbon, with R_{int} of 19 ± 1 Ω and achieved the highest power density of 11 W m^{-3}. Based on lab-scale experiments (scaling-up factors not considered) energy savings of up to 7 % (AnAOB), 44 % (AOB) and 475 % (EAB) (positive energy balance), compared to conventional nitrification, are projected from the applications of BEAO in wastewater treatment plants.

1. Introduction

Disposal of ammonia nitrogen into bodies of water can cause adverse effects. This is particularly important for high-strength nitrogen wastewater, such as wastewater from dewatering of digested biosolids (Johnson et al., 2018), landfill leachate (Cano et al., 2019), swine manure (Xu et al., 2019) and vinasse from ethanol production (España-Gamboa et al., 2011). Thus wastewater treatment is necessary prior to discharge into natural water bodies.

Biological treatment is usually applied for nitrogen removal from wastewater and is conventionally based on nitrification followed by denitrification (Cano et al., 2020; Lee et al., 2022). In nitrification, ammonia-oxidizing bacteria (AOB) and nitrite-oxidizing bacteria (NOB) sequentially convert ammonia (NH_3) to nitrite (NO_2^-), and nitrite to nitrate (NO_3^-), respectively (Daims et al., 2016; Lam and Kuypers, 2011):

$$NH_3 + 1.5\ O_2 \rightarrow HNO_2 + H_2O \quad (1)$$

$$\Delta G^\circ = -278\ \text{kJ mol}^{-1}$$

$$NO_2^- + 0.5\ O_2 \rightarrow NO_3^- \quad (2)$$

$$\Delta G^\circ = -82\ \text{kJ mol}^{-1}$$

The conventional nitrification process requires a high amount of oxygen (4.57 g O_2 g NH_4^+-N^{-1}) to support the growth of strictly aerobic nitrifying bacteria (Daims et al., 2016; Sharma and Ahlert, 1977). However, the aeration system accounts for 50 % to 90 % of the total electricity consumed within a wastewater treatment plant (WWTP) (about 0.6 kWh m^{-3}) and amounts to 15 % to 49 % of the total operating costs of WWTPs (Drewnowski et al., 2019; Gu et al., 2017; Gude, 2015). Hence the energy budget of conventional wastewater treatment technologies relying on nitrification process represents a major challenge in terms of sustainability.

Other technologies involving nitrogen towards less energy demand and circular economy are under development. Partial nitrification followed by the anaerobic ammonia oxidation (anammox) process has been considered for the reduction of energy consumption in WWTPs (Kartal et al., 2011; Zekker et al., 2021). In comparison to conventional nitrification, 60 % less oxygen is necessary, since ammonia nitrogen is only partially oxidized to nitrite (Cao et al., 2017). In this regard, strategies to suppress the activity of nitrite-oxidizing bacteria (NOB) and to intensify the activity of anammox bacteria are under development, aiming at industrial and municipal wastewater treatment (Zekker et al., 2011, 2014). Another approach under development with different technology readiness levels is the nitrogen recovery from wastewater for re-use in agriculture. Such technologies include struvite formation and ammonia stripping, among others (Chrispim et al., 2020; Nancharaiah et al., 2016).

Alternatively, ammonia has been gaining an increasing attention as a carbon-free energy source (Engelberth et al., 2021; Yüzbaşıoğlu et al., 2022). Based on Eqs. (1) and (2), up to 5.5 Kwh per g NH_4^+-N and 1.6 Kwh per g NO_2^--N^{-1} are theoretically available from ammonia and nitrite oxidation, respectively (Daims et al., 2016; Lam and Kuypers, 2011). Thus, harvesting energy from ammonia within wastewater can contribute to reduce the energy demand of WWTPs. This approach has not yet been successfully implemented though.

In terms of bacteria metabolism, the oxidation of ammonia nitrogen to nitrite by AOB occurs in a two-step process. Firstly, a membrane-bound enzyme, ammonia monooxygenase (AMO), catalyzes the oxidation of ammonia to hydroxylamine (NH_2OH). Secondly, in the periplasmic space, hydroxylamine is oxidized to nitrite by the hydroxylamine oxidoreductase (HAO), releasing four electrons that are channeled through a cytochrome system to the ubiquinone pool. Then, the electrons are partitioned to support the reaction by AMO (reverse electron transfer), and to generate a proton gradient during the electron transport chain up to the terminal electron acceptor (oxygen) (Whittaker et al., 2000; Sayavedra-Soto and Arp, 2014). During the second step of nitrification, nitrite is oxidized to nitrate by NOB through the nitrite oxidoreductase (NXR), releasing two electrons to the electron transport chain (Poughon et al., 2001; Hemp et al., 2016).

Hence, conventional biological processes cannot directly harvest energy from ammonia because the oxidation mechanisms of bacteria are coupled to an intracellular respiratory chain with oxygen as the terminal electron acceptor (Hemp et al., 2016; Poughon et al., 2001; Sayavedra-Soto and Arp, 2014; Whittaker et al., 2000).

Bioelectrochemical systems (BES) were developed over the last decades centered on the demonstrated ability of coupling the intracellular electron donor oxidation with an extracellular electron acceptor. The microbial fuel cells (MFC) utilize such ability to convert chemical energy of biodegradable substrates directly into electric energy (electricity). The activity of electroactive bacteria (EAB) generates electricity in this system by transferring electrons to insoluble electron acceptors (such as Fe (III) and Mn (IV) oxides and electrodes) through their outer membranes in a process known as extracellular electron transfer (EET). Electrons transferred by EAB to an electrode (anode) migrate through an external circuit to a second electrode (cathode). On the cathode, the terminal electron acceptor (oxygen) is reduced. Hence, the electron donor oxidation is spatially separated from the terminal electron acceptor reduction and electric current is generated (Lovley and Holmes, 2022).

Microbial fuel cell's studies have mostly aimed at oxidizing organic carbon and not ammonia. The first contribution related to energy generation associated with ammonia oxidation in a BES was provided by He et al. (2009), and it was only recently that the occurrence of this process in completely anaerobic conditions was clearly demonstrated (Shaw et al., 2020; Vilajeliu-Pons et al., 2018). The bioelectrochemical ammonia oxidation (BEAO) is not an aerobic process since bacteria rely on the anode as electron acceptor and not on oxygen. Thus aeration is not intrinsically necessary. Moreover, the process may lead to the generation of electricity (Nolasco et al., 2022; Cano, 2020). Thus, it is considered a more sustainable technology for nitrogen treatment (Anastas et al., 2021). If the process can be controlled at a high rate, its combination with other energy generating processes from organic matter may represent a breakthrough in the energy balance of WWTPs.

To date, the studies published in the literature regarding BEAO have proposed different strategies for stimulating electroactive ammonia-oxidizing activity (Joicy et al., 2019; Koffi and Okabe, 2021; Ruiz-Urigüen et al., 2019; Tang et al., 2017). This plethora of studies has produced a various results without a consensus regarding the BEAO mechanisms (as summarized next).

Hassan et al. (2018) applied the MFC for energy generation from landfill leachate treatment and observed power densities increasing with the increment of NH_4^+-N up to 240 mg L^{-1}. In order to corroborate whether NH_4^+-N acted as anodic fuel to generate electricity, a synthetic wastewater having NO_2^- − N/NH_4^+-N = 1.32 without organic carbon was used in the MFC. In this condition, power density increased in the initial five successive batch cycles but rapidly decreased after that.

Tang et al. (2017) also showed that the substitution of an organic substrate for NH_4^+-N after the growth of conventional EAB leads to the production of electric current. The dominance of the *Nitrosomonadaceae*, *Ignavibacteriaceae,* and *Geobacteraceae* bacterial families was observed under such condition. This finding suggests that microbial communities from biofilms enriched with EAB can adapt to oxidize ammonia, maintaining a certain level of current generation in the absence of organic carbon.

Autotrophic bacteria have been associated with BEAO independently of heterotrophic EAB presence. However, the resulting reaction products were found to be different from the products expected to be generated based on the known enzymology of these bacteria (Daims et al., 2016). For instance, bacteria from the genus *Nitrosomonas* have now been associated with ammonia oxidation combined with current generation and production of NO_3^- (He et al., 2009) and N_2 (Zhan et al., 2014). Similarly, Qu et al. (2014) achieved ammonium oxidation with a microbial community dominated by *Nitrosomonas europaea* and proposed anode as the electron acceptor in a dual chamber microbial electrolysis cell (MEC). However, instead of nitrite, nitrate was reported as the main product of ammonium oxidation.

In a study focusing on the hydrogen production on the cathode with ammonia as electron donor on the anode, biotic and abiotic conditions were tested (Zhan et al., 2014). Current generation was achieved only when bacteria was present, with dominance of *Stenotrophomonas* (13.1 %), *Nitrosomonas* (12.9 %), *Comamomas* (10.8 %) and *Paracocus* (10.6 %). In this condition, accumulations of nitrite or nitrate were not observed.

Other studies have employed anammox bacteria (AnAOB) in BES (Koffi and Okabe, 2021; Zhu et al., 2016). In conventional anammox process, autotrophic bacteria belonging to the phylum of Planctomycetales rely on nitrite as (1) electron acceptor to oxidize ammonia nitrogen to dinitrogen (N_2); and (2) as electron donor for CO_2 reduction to biomass (Strous et al., 1999; Kartal et al., 2011). However, in a BES enriched with Ca. Brocadia and Ca. Scalindua, the successful ammonia oxidation and generation of current was reported in absence of NO_2^- (Shaw et al., 2020).

Jadhav and Ghangrekar (2015) observed ammonia removal by applying a voltage to the cathode (+ 0.67 V vs Ag/AgCl), and proposed the occurrence of anammox coupled to current generation. Furthermore, Zhu et al. (2016) controlled the anodic potential of a BES to − 0.5 V vs. Ag/gCl, and observed ammonia removal efficiency increased by at least 29.2 % compared to a conventional anammox reactor without electrodes.

Enrichment of *Acidimicrobiaceae* sp. A6 in a MEC also resulted in ammonium oxidation. The results showed that over time majority of cells were in the bulk liquid, and not attached to the anode, requiring the addition of 9,10-anthraquinone-2,6-disulfonic acid (AQDS) as soluble electron shuttling compound (Ruiz-Urigüen et al., 2019). These results suggest other functional groups of bacteria potentially participate in mechanisms utilizing EET in addition to EAB, AOB and AnAOB.

At least three functional groups of bacteria have been associated with ammonia oxidation combined with EET in BES (He et al., 2009; Shaw et al., 2020; Koffi and Okabe, 2021). The reported studies indicate that the parameters of the basic BEAO process and the elucidation of the enzymatic mechanisms responsible for the process have not been fully demonstrated. Different molecular mechanisms and limiting factors associated with the bacteria enzymology may yield different performances of energy generation and ammonia oxidation in BES. However, direct comparison between studies may not be conclusive to determine the performance of different bacterial groups, because of different conditions, materials and configurations utilized in each study. Furthermore a significant number of studies have relied upon energy input to maintain the electric potential difference at a determined level (Hussain et al., 2016; Joicy et al., 2019; Koffi and Okabe, 2021; Pous et al., 2021; Qu et al., 2014; Siegert and Tan, 2019; Zhan et al., 2014; Zhu et al., 2021). Hence, the link between the spontaneous microbially-mediated reactions and energy production in such BES is unclear.

Therefore, it is necessary to identify the pathway(s), limiting variables, elements of microbial ecology, and the degree to which each group of bacteria can produce energy. In this context, the present study sought to investigate BEAO by different functional bacterial groups enriched in mixed cultures and the contributions of these different functional groups on the overall performance of a MFC.

MFCs fed with synthetic wastewater were inoculated and selectively enriched with heterotrophic EAB, AOB, and AnAOB. Then, the potential EET mechanisms and identified limiting factors by each microbial community were elucidated based on a comparative analysis of the levels of electricity generation, bioelectrochemical properties and operating parameters. Based on the findings, the study discussed conditioning and operating strategies to shape microbial ecology towards more efficient BEAO, and projected the range of energy savings regarding the process application in a WWTP.

2. Experimental procedures

2.1. Microbial fuel cell prototype setup

The tubular concentric dual-chamber MFC (Fig. 1) consisted of a 1-L styrene-acrylonitrile resin tube with an external anodic chamber and an internal cathodic chamber separated by a Nafion 117 membrane (17 × 22.2 cm). The cation exchange membrane was selected for the correct interpretation of the results, avoiding crossover and migration of nitrite and nitrate between chambers. The inner and outer chambers were, respectively, filled with 143.1 ± 3.9 g and 177.6 ± 7 g of granular activated carbon (GAC, Tobasa BioIndustrial, Brazil), with a diameter between 2 and 3.36 mm (mesh 6–10) used as tridimensional electrodes. A stainless steel AISI 304 mesh 10 (Central Mesh, Brazil, containing about 18.5 % Cr and 10 % Ni) with 0.56 mm wire diameter was used for collecting current. The distance between the anode and cathode columns was around 6 mm. The net volumes of the anodic and cathodic chambers were 430 mL and 184 mL, respectively. Details of the system configuration and dimensions can be found in the Fig. S1 and detailed information about the manufacture of each component of the MFC is presented in Cano et al. (2021).

2.2. Wastewater

Two synthetic wastewater formulations were used, simulating pretreated vinasse, a by-product from the distillation of ethanol following fermentation of carbohydrates from sugarcane. The organic wastewater was used for enriching the heterotroph bacteria and contained 2.5 g COD L^{-1}, 437.5 mg NH_4^+-N L^{-1} with a conductivity of 830.3 ± 114.6 mS m^{-1}. The second formulation, named inorganic wastewater, contained 437.5 mg NH_4^+-N L^{-1} with a conductivity of 829.2 ± 109.4 mS m^{-1}. Both wastewaters were complemented with 1 mL L^{-1} solution of trace elements. Detailed information on the composition of the organic and inorganic wastewater and trace elements are included in the Supplementary Material (SM, Table S1).

2.3. Inocula and operating conditions

Four MFCs (MFC-EAB, MFC-AOB, MFC-AOB2, and MFC-AnAOB) were independently operated with a continuous flow rate of 0.307 L d^{-1} and HRT of 33.6 h (anode chamber), at room temperature (23 °C) with external resistance (R_{ext}) of 300 Ω (compatible with EAB growth and stable operation based on previous assessment). The recirculation of the anode effluent to the cathode effluent was applied to the development of a biocathode and complementary treatment. For the MFC-AOB2 system, the anode effluent was recirculated through the cathode chamber by direct connection between the anode and cathode chambers at the bottom of the reactor (Fig. 2a). Hence, in this configuration a pump was not necessary to feed the cathode chamber, which is relevant for the large-scale application of compact MFC stacks. In the case of the MFC-EAB, MFC-AOB, and MFC-AnAOB systems, the recirculation process occurred by external pumping of the anode effluent into the inner chamber (Fig. 2b). This prevented diffusion of oxygen from the cathode chamber to the anode. Laboratory air was directly supplied in the cathode chamber at a flow rate of 2 LPM and 1 LPM when the organic and inorganic wastewaters, respectively, were used. The

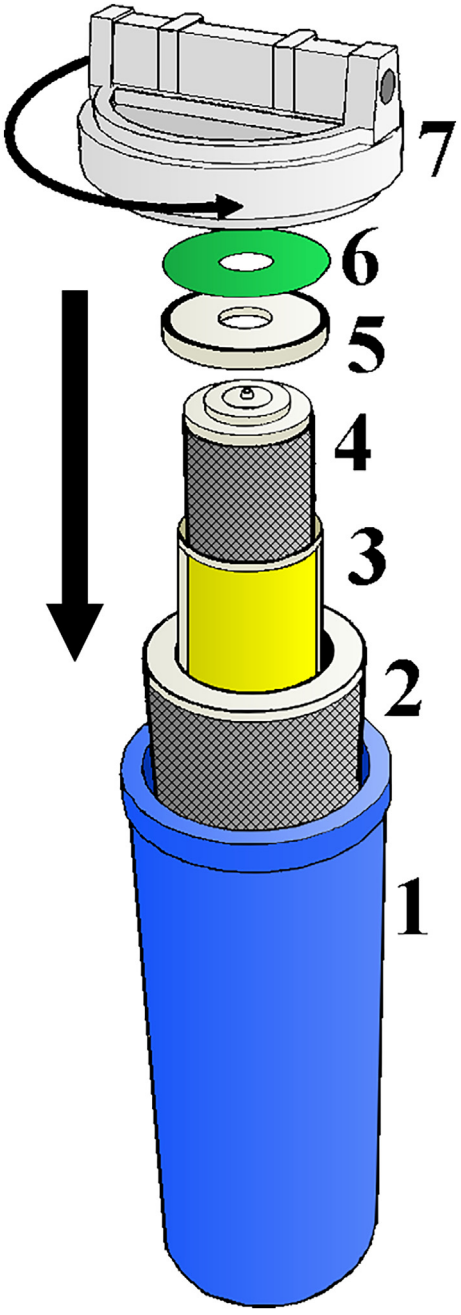

Fig. 1. Tubular concentric dual-chamber MFC consisting of a (1) styrene acrylonitrile resin tube; (2) external stainless steel mesh; (3) PVC support with Nafion 117; (4) internal stainless steel mesh; (5) Nafion 117 support cap; (6) silicone foil for sealing; and (7) reactor cap.

different airflow rates were defined on the basis of theoretical oxygen demand to oxidize organic matter (COD) and/or ammonia to nitrate (4.57 g O_2 per g NH_4^+-N) (Sharma and Ahlert, 1977).

The anode chamber of MFC-EAB was inoculated with activated sludge (2.5 g VSS L^{-1}) from a municipal WWTP. 640 mL of the mixed liquor was concentrated by decantation to a final volume of 100 mL (16 g VSS L^{-1}). The concentrated biomass was diluted with the organic synthetic wastewater to a final volume of 430 mL and placed inside the anode chamber. After 24 h of inoculation, the reactor was continually fed with organic wastewater to promote the growth of electroactive anodic bacteria. After 75 days of operation, sulfate (SO_4^{2-}) was removed from the organic wastewater feed medium to minimize growth of sulfate-reducing bacteria. This operational condition lasted 33 days. Thereafter, the organic carbon

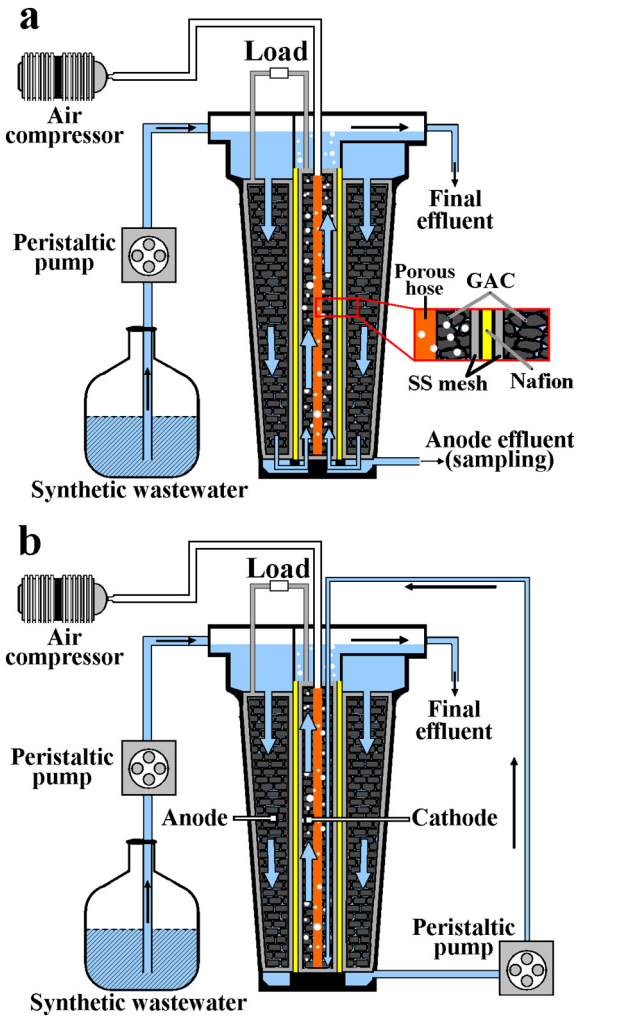

Fig. 2. Scheme illustrating laboratory tubular MFC with anode effluent recirculation to the cathode (a) by an internal connection between the anode and cathode chambers; and (b) by external pumping.

concentration of the influent wastewater was reduced to 1 g COD L^{-1}. After 28 days, the organic wastewater was replaced by inorganic wastewater, and the reactor was operated for 64 days to assess whether the enriched EAB biofilm was able to adapt to the inorganic substrate (NH_4^+) used as the electron donor. The MFC-EAB is referred to MFC-EAB (organic) and MFC-EAB (inorganic) when fed with organic and inorganic wastewater, respectively.

The anode chambers of MFC-AOB and MFC-AOB2 were inoculated with 107 mL of concentrated biomass (15 g VSS L^{-1}) collected from a laboratory bioreactor operating more than five years with an enriched community of nitrifiers (AOB and NOB) (Brotto et al., 2018). The anode chamber of MFC-AnAOB was inoculated with biomass collected from a side-stream deammonification moving bed biofilm reactor operating for over three years (Ma et al., 2015). Each biomass was diluted with inorganic wastewater to a final volume of 430 mL and placed inside the respective reactor.

The MFC-AOB, MFC-AnAOB, and MFC-AOB2 were continually fed with inorganic wastewater after 24 h of inoculation. MFC-AOB and MFC-AnAOB were operated under this condition for 98 days, while MFC-AOB2 was operated under the same condition for 163 days. Then, to assess the influence of SO_4^{2-} over the process as an alternative electron acceptor, MFC-AOB and MFC-AnAOB were operated without SO_4^{2-} in the inorganic wastewater for 58 days, while for MFC-AOB2 it lasted 46 days.

After reaching a steady-state condition (daily current generation variation <5 % and < 10 % within 7 d), all the reactors fed with inorganic substrate were operated for 7 days with inorganic wastewater in the absence

of NH_4^+-N aiming to evaluate the relation between NH_4^+-N oxidation and current generation.

Additionally, a control abiotic reactor (same configuration and materials) was operated in batch mode (triplicate) for 33 h with the inorganic wastewater in the anode chamber and phosphate buffer solution (0.1 M, pH 7) in the aerated cathode chamber. The reactor was maintained in closed circuit (R_{ext} = 300 Ω) to assess whether non-biological oxidation of ammonia contributed to current generation. The results were also used to measure the NH_4^+-N removal by transfer from anode to cathode chambers through the cation exchange membrane (CEM).

2.4. Electrochemical and physicochemical measurements

The cell potential difference (voltage, V) was recorded daily using a True RMS digital multimeter and converted to current (I) according to Ohm's Law ($I = V/R_{ext}$). The anode potential was measured using Ag/AgCl reference electrodes (KCl saturated, +200 mV vs Standard Hydrogen Electrode, SHE) placed in the anode chamber. The current densities were calculated dividing the current by the net anodic volume (0.43 L).

The polarization curves were obtained and internal resistances were calculated according to Logan (2012) with methods detailed in (Cano et al., 2021). The volumetric power density was normalized to the net anodic volume. Coulombic efficiency (CE) was calculated by dividing the coulomb output by the total coulomb input. The total coulomb input was derived from NH_4^+-N for the reactors fed with inorganic wastewater (details in SM, Section 4). The calculation was performed based on four electrons released from the oxidation of NH_2OH to NO_2^- or via hydrazine (N_2H_4) oxidation to N_2 (Kartal et al., 2011; Vilajeliu-Pons et al., 2018).

Liquid samples were collected at regular intervals (twice a week) from the anode influent, anode effluent, and cathode effluent (final effluent). NH_4^+-N removal rates based on the comparison between influent and anode effluent consider both NH_4^+ oxidation and migration across the CEM. Thus, NH_4^+-N oxidation rates based on influent and effluent nitrite (NO_2^--N) and nitrate (NO_3^--N) concentrations were used to assess the biological activity in the anode chamber. The NH_4^+-N concentration and pH were determined using an ion selective electrode meter (Orion Dual Star pH/ISE Dual Channel - 2,115,000 series, Thermofisher Scientific, USA), equipped with an ammonium ion-electrode. Nitrite (NO_2^--N), nitrate (NO_3^--N) and sulfate (SO_4^{2-}) concentrations were determined using an ion chromatographer ICS 2100 (Thermofisher Scientific, USA) equipped with the IonPac AS-18 column. The COD was determined spectrophotometrically according to the closed reflux method (APHA, 2017). All chemicals utilized in this study were obtained from companies in the USA or Brazil and met the American Chemical Society (ACS) grade or had higher purity.

2.5. Statistical analysis

All the data used for the comparative analyses of the reactors were tested for normality by the Kolmogorov-Smirnov test. ANOVA ($\alpha = 0.05$) was used for the data with a normal distribution to test the differences between the mean values. When differences were found, the *t*-test for two samples was used ($\alpha = 0.05$) to verify the difference between two reactors. For the data that did not present a normal distribution, median values were tested using the non-parametric Kruskal-Wallis ($\alpha = 0.05$) and Mann-Whitney ($\alpha = 0.05$) tests. The results obtained in each test are presented in the SM (Section 12). The Minitab® 19 software was used for conducting the statistical tests.

2.6. Energy savings calculations

Energy savings were calculated based on the energy generated by each MFC and the theoretical energy demand of conventional nitrification. The energy demand for nitrification was calculated based on the standard aeration efficiency of 0.24 kWh kg O_2^{-1} (Colacicco and Zacchei, 2020; Kim et al., 2020) and the oxygen demand for production of NO_2^--N and NO_3^--N at the concentrations observed for each MFC unit. The oxygen demand was calculated using 4.57 kg O_2 kg N^{-1} for complete NH_4^+ oxidation to NO_3^- and 3.43 kg O_2 kg N^{-1} for incomplete oxidation to NO_2^- (neglecting biomass synthesis) (Sharma and Ahlert, 1977). The calculations are presented in detail in the SM (Section 7).

2.7. Characterization of the microbial communities

To characterize the structure of the microbial community for the MFC-EAB reactor fed with organic substrate, the biofilm attached to the anode was sampled right before decreasing the COD of the synthetic substrate. For the MFC-EAB with NH_4^+ substrate, MFC-AOB, MFC-AnAOB, and MFC-AOB2, the biofilm samples were collected from the anode at the end of the experiment. Immediately after collection, the biomass was separated from the GAC by vortexing in 7 mL of deionized water for 1 min. The biomass in the solution was concentrated by centrifuging at 16.1 × 1000 g for 10 min at 4 °C. The resultant material was then stored at −80 °C until DNA extraction. The protocols utilized for DNA extraction, next-generation 16S rRNA amplicon sequencing and further post-sequencing bioinformatic analysis are described in Obata et al. (2020). Amplicon sequencing data are publicly available at NCBI (BioProject ID: PRJNA803873).

In our study, the utilization of the terms EAB, AOB, and AnAOB refer to previous knowledge and terminology applied in the field of biological and bioelectrochemical processes. AOB refers to autotrophic bacteria that aerobically oxidize NH_4^+–N to NO_2^-–N (nitrification), belonging to the β-Proteobacteria and γ-Proteobacteria subclasses, such as *Nitrosomonas* and *Nitrosospira* (Chen et al., 2023). AnAOB refers to anammox bacteria, which can convert NH_4^+–N and NO_2^-–N into N_2 under anaerobic conditions, and belong to the phylum Planctomycete, such as *Candidatus* Brocadia and *Candidatus* Kuenenia (Chen et al., 2023). EAB are widely considered as bacteria that can exchange electrons with electrodes (Paquete et al., 2022). A strict definition has not yet been fully defined in the field of bioelectrochemical ammonia oxidation. Thus, the ability of EET by AOB and AnAOB implies these bacteria are EAB as well. However, to facilitate discussion towards different functional groups, in our study EAB refers specifically to heterotrophic anode-respiring bacteria, such as *Geobacter* and other the dissimilatory metal-reducing bacteria (Philips et al., 2016).

3. Results and discussion

3.1. Ammonia oxidation performance

The MFC-EAB reactor fed with organic substrate achieved COD removal rate of 1.38 ± 0.38 kg m^{-3} d^{-1} corresponding to a removal efficiency of 77.3 ± 6.8 %, and coulombic efficiency (based on COD) of 2.74 ± 0.63 %. The average NH_4^+-N removal from the anode chamber was 51.2 ± 9.8 %, with mean removal rate of 187.5 ± 94.0 g NH_4^+-N m^{-3} d^{-1}. Low concentrations of NO_2^--N (0.7 ± 1.1 mg L^{-1}) and NO_3^--N (2.6 ± 1.9 mg L^{-1}) were observed in the anode effluent, which suggests ammonia oxidation did not occur at high rate or was followed by heterotrophic denitrification (Fig. 3).

The NH_4^+-N removal rate of MFC-EAB (organic) was not significantly different ($p = 0.887$) from the NH_4^+-N transfer rate through the Nafion membrane observed in the abiotic reactor (194.3 ± 84.5 g N m^{-3} d^{-1}, Fig. S15). CEMs, such as Nafion, are permeable by NH_4^+. This suggests that in our study the removal rate of NH_4^+-N of MFC-EAB (organic) was mostly associated with the transfer of ammonia to the cathode chamber through CEM. This is in accordance with results frequently reported in studies with BES fed with organic substrate, in which NH_4^+-N is transferred through CEM (Leong et al., 2013).

In the absence of organic carbon, the NH_4^+-N removal rates of MFC-EAB (inorganic), MFC-AOB, MFC-AnAOB were not significantly different ($p = 0.418$) from those obtained for the MFC-EAB fed with organic wastewater. Nevertheless, only the reactors fed without organic carbon (MFC-EAB (inorganic), MFC-AOB, MFC-AOB2, and MFC-AnAOB) presented NO_2^--N and NO_3^--N accumulation in the anode effluent. This resulted in NH_4^+-N oxidation rates of 66 ± 19 g NH_4^+-N m^{-3} d^{-1}, 83 ± 25 g NH_4^+-N m^{-3} d^{-1},

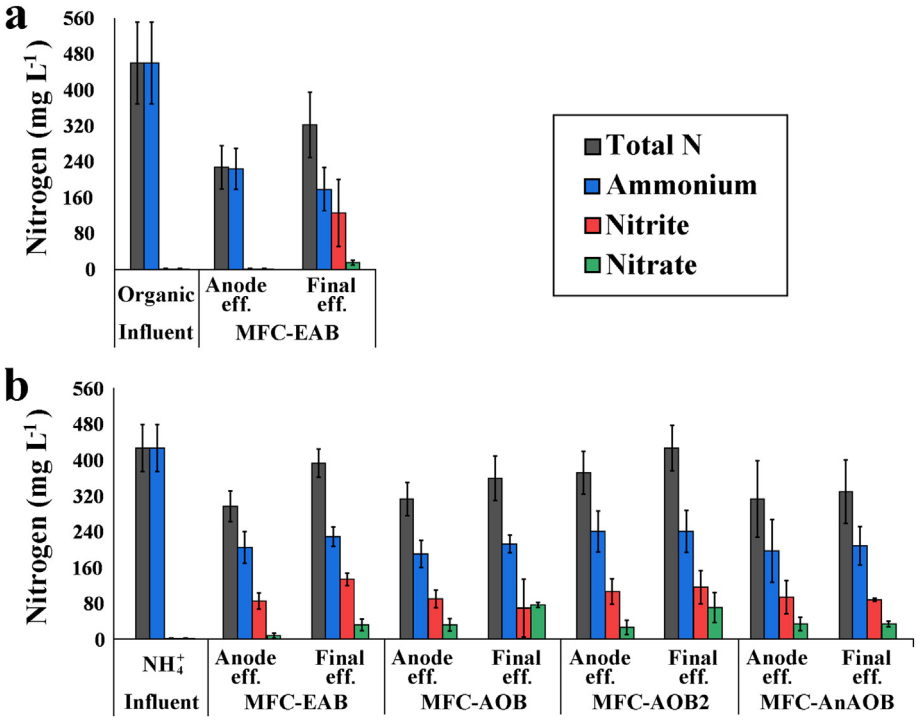

Fig. 3. Nitrogen profile, including average NH_4^+-N, NO_2^--N, NO_3^--N and total N for influent, anode chamber effluent, and final effluent (cathode chamber effluent) of (a) MFC-EAB with organic substrate and (b) MFC-EAB, MFC-AOB and MFC-AnAOB with inorganic (NH_4^+) substrate.

93 ± 34 g NH_4^+-N m^{-3} d^{-1} and 82 ± 35 g NH_4^+-N m^{-3} d^{-1} for MFC-EAB (inorganic), MFC-AOB, MFC-AOB2 and MFC-AnAOB, respectively. Average concentrations higher than 80 mg NO_2^--N L^{-1} were observed for all reactor fed with inorganic wastewater, while concentrations of 7.7 ± 0.5 mg NO_3^--N L^{-1}, 32.0 ± 14.4 mg NO_3^--N L^{-1}, 26.2 ± 15.8 mg NO_3^--N $L^{-1}$and 32.8 ± 16.4 mg NO_3^--N L^{-1} were observed for MFC-EAB (inorganic), MFC-AOB, MFC-AOB2 and MFC-AnAOB, respectively (Fig. 3).

Nitrite and nitrate are negatively charged ions and are not able to migrate from the cathode chamber to the anode chamber through the CEM. This means that the presence of oxidized nitrogen species in the anode chamber (Fig. 3) was a result of NH_4^+-N oxidation in the same chamber. NO_2^- was the main final product of the reactions in the MFC-EAB (NH_4^+ substrate), MFC-AOB and MFC-AnAOB reactors as also reported elsewhere (He et al., 2009). The reactions leading to NO_2^- accumulation will be further discussed considering the microbial community structure in the following sections.

There was a significant decrease in pH ($p < 0.001$) after NH_4^+-N oxidation in the anode chamber of all reactors compared to the pH of the influent (see the Fig. S14). The decrease of pH is another indication of chemolithoautotrophic ammonia oxidation (Chandran and Smets, 2000).

Regarding total nitrogen removal, the global removal (includes anode and cathode processes) of MFC-EAB (organic), MFC-EAB (inorganic), MFC-AOB, MFC-AOB2, and MFC-AnAOB were, respectively, 33 ± 16 %, 17 ± 9 %, 25 ± 13 %, 15 ± 12 %, and 25 ± 14 %. Specific processes relating the microbial community on the anode and the cathode with nitrogen removal are, respectively, discussed in the following sections and in the SM (Section 8). Additionally, nitrogen assimilation processes may have contributed to nitrogen removal in all MFCs. Such processes include assimilatory nitrate reduction, assimilatory nitrite reduction and ammonia assimilation. Nitrogen assimilation is closed related to the biomass synthesis. Hence, nitrogen assimilation is expected to increase with bacterial growth rate (Han and Zhou, 2022; Kuypers et al., 2018). This is consistent with the higher nitrogen removal observed by MFC-EAB (organic), since, in addition to NH_4^+, organic carbon was available as electron donor for bacteria growth. However, compared to high rate aerobic processes, nitrogen assimilation in MFC is not considered a primary removal route because of relatively low growth rates of EAB (Oksuz and Beyenal, 2021).

3.2. Current generation association with ammonia

The MFC-AOB and MFC-AnAOB reactors presented average voltages of 137 ± 38 mV and 150 ± 37 mV, respectively. Regarding to MFC-EAB, when the organic substrate was substituted for the NH_4^+ substrate, the voltage decreased from >700 mV to 283 mV. This was a result of increase in anode potential (Fig. 4a).

To evaluate whether the current generated was related to NH_4^+-N, all reactors were fed with the inorganic wastewater without NH_4Cl for 7 days. An immediate decrease was observed in the current of MFC-EAB, MFC-AOB, and MFC-AOB2, and there was an increase in the current when NH_4Cl was applied to the system again (Fig. 4b). The conductivity of the wastewater without NH_4Cl was 485 ± 8.12 mS m^{-1}, which was around 1.7 fold lower than the wastewater with NH_4Cl. Nevertheless, the currents with NH_4Cl were between 2.5 and 3.3 fold higher compared to the ones observed without NH_4Cl. Hence, the sole increase and decrease in conductivity do not explain the measured currents as expected by Ohm's law. This observation is similar to the one reported by Vilajeliu-Pons et al. (2018) and confirms the relationship between NH_4^+-N and current generation in our study.

Current generation and NH_4^+-N oxidation were not observed in the abiotic reactor. Thus, unlike what was proposed by Chen et al. (2014), generation of current through a purely electrochemical reaction (non-biological) did not contribute to current in BEAO-MFCs.

Several studies regarding the BEAO have relied on energy input to induce the process (Hussain et al., 2016; Joicy et al., 2019; Pous et al., 2021; Qu et al., 2014; Siegert and Tan, 2019; Zhan et al., 2014; Zhu et al., 2021). In our study, external energy was not used to control the electrode potential or to generate an electrostatic field. The current was intrinsically generated by bacteria.

With 300 Ω R_{ext}, MFC-EAB achieved average current densities of 3.59 ± 1.21 A m^{-3} while for MFC-AOB, MFC-AOB2, and MFC-An-AOB it ranged from 1.00 to 1.16 A m^{-3}. The higher current of MFC-EAB resulted in

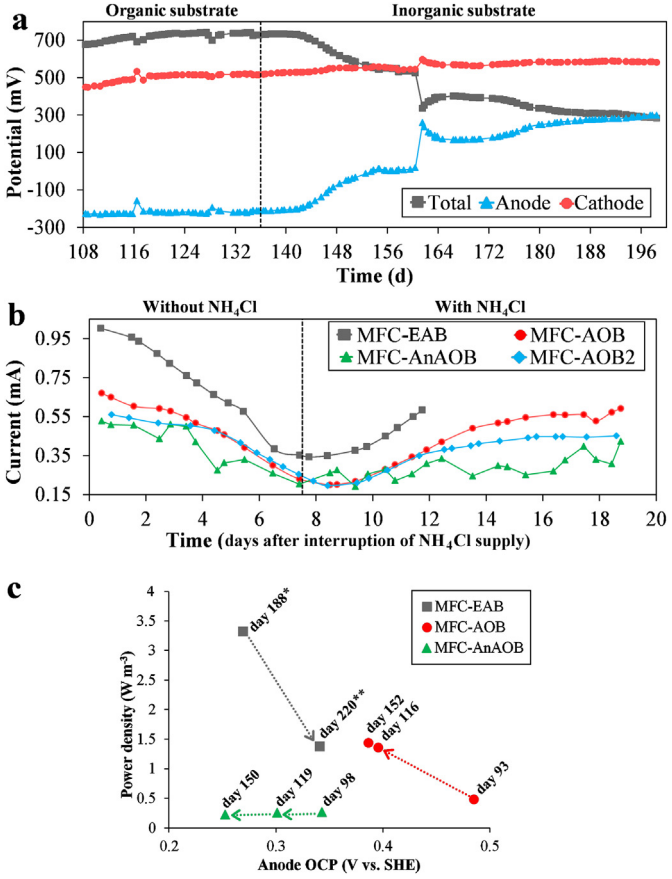

Fig. 4. (a) MFC-EAB potential difference (■), anode potential (△) and calculated cathode potential (○) obtained via the feeding of the system with organic and NH_4^+ substrates; (b) current generation of MFC-EAB (inorganic) (■), MFC-AOB (○), MFC-AnAOB (△) and MFC-AOB2 (♦) regarding the presence of ammonium at the end of the experiment, timeline is relative to interruption of NH_4Cl supply; (c) Evolution of power density in relation to the anode OCP for MFC-EAB (■), MFC-AOB (○) and MFC-AnAOB (▲) based on the polarization curves obtained from the operation for *53 days and **83 days after the beginning of the NH_4^+ substrate phase.

coulombic efficiency of 14.1 ± 4.5 % and normalized energy recoveries of 0.661 ± 0.4 kWh per Kg of oxidized N. MFC-AOB, MFC-AOB2, and MFC-An-AOB achieved CE between 5 % and 7 %, with normalized energy recoveries ranging from 0.049 to 0.063 kWh per Kg of oxidized N (Table 1).

Furthermore, despite the similar current densities under 300 Ω R_{ext}, substantially different results were observed when external resistance equalled the internal resistance (in polarization curve tests, Table 1). This reveals that apart from of MFC-AnAOB the MFC performances were limited by the high external resistance. The analysis of polarization curves also showed the evolution of the maximum power density and anode potential in open circuit mode for each reactor during the operation (Fig. 4c). Despite similar NH_4^+ removal rates, each reactor exhibited diverse levels of energy generation.

The MFC-EAB (inorganic) and MFC-AOB reactors showed comparable power densities at the end of the experiment. The MFC-AnAOB reactor presented a maximum power density that was at least six-fold lower than that of the MFC-AOB reactor. Pathways for current generation in the anode and implications for the performance of each reactor are discussed in the following sections. Details of the cathode chamber performance are presented in the SM (Section 8).

3.3. Adaptation of MFC-EAB to oxidize NH_4^+-N

The most abundant genus in the MFC-EAB fed with organic substrate was *Geobacter* (24.7 %), followed by *Lactococcus* (7.4 %), *Acinetobacter* (4.3 %), *Arcobacter* (4.1 %), and bacteria belonging to the *Synergistaceae* (4.1 %), *Sphaerochaeta* (4.1 %), *Desulfobulbus* (3.2 %), the order Lactobacillales (1.9 %), and *Desulfovibrio* (1.8 %) family (Fig. 5).

Geobacter, *Acinetobacter*, *Lactococcus*, *Arcobacter*, *Desulfobulbus* and *Desulfovibrio* are EAB which have been reported in MFCs fed with organic compounds such as glucose, glycerol, acetate, pyruvate, lactate and propionate (Fedorovich et al., 2009; Hodgson et al., 2016; Li et al., 2018). The order Lactobacillales presents EAB species (e.g. *Trichococcus* sp.) (Barbosa et al., 2018). Considering the aforementioned bacteria, most of the community members (55.7 %) were potentially active heterotrophic EAB.

When the MFC-EAB reactor was fed with NH_4^+ substrate for 64 days, a considerable change was observed in the microbial community structure and composition. The relative abundance of *Geobacter* decreased to 4.5 %, and other EAB were not found. The following groups were also detected: *Burkholderiaceae* (12 %), *Denitratisoma* (9.1 %), *Anaerolineaceae* (7.5 %), *Longilinea* (4.9 %), and *Leptolinea* (3.8 %). Interestingly, AOB, AnAOB, and NOB were not found in MFC-EAB.

Denitratisoma are heterotrophic denitrifying bacteria (Wang et al., 2019). *Burkholderiaceae* are also denitrifying bacteria that are associated with various phenolic compounds (Vashi et al., 2019). The presence of these bacterial groups was likely supported by the endogenous decay of the community previously grown when organic carbon was available. The presence of these bacteria has been reported elsewhere in similar circumstances (Joicy et al., 2019; Zhang et al., 2019a).

Anaerobic digesters and the BES have been found to contain *Longilinea* and *Leptolinea*. These bacteria are strictly anaerobic heterotrophs that are known to convert carbohydrates and amino acids into acetate, lactate, and hydrogen (Zhang et al., 2017). Although neither *Longilinea* nor *Leptolinea* can produce current, they may have had a syntrophic association with *Geobacter* sp.. The occurrence of a syntrophic growth suggests that the organic compounds derived from the bacterial decay or adsorbed in the GAC may have contributed to the current generation as reported elsewhere (Caizán-Juanarena et al., 2020). This could have been especially important during the first 7 days after switching from the organic substrate to NH_4^+ substrate. The current generation was stable at an elevated level during this period (Fig. 4a).

After substituting the organic wastewater for the NH_4^+ one, the internal resistance of MFC-EAB slightly increased from 12 Ω to 18–21 Ω. This means that despite the changes in microbial community, the anodophilic activity persisted. On the contrary, Hussain et al. (2016) reported considerable

Table 1
Summary of results achieved by each MFC in this study regarding volumetric current density with 300 Ω R_{ext} and when R_{ext} equalled R_{int} in polarization curve, coulombic efficiency based on N, and normalized energy recovery based on ammonia removed or oxidized in the anode chamber. Results expressed as mean ± standard deviation.

MFC	Current density (A m^{-3})		CE based on N (%)	Normalized energy recovery	
	R_{ext} = 300 Ω	R_{ext} = R_{int}		kWh kg $N_{removed}^{-1}$	kWh kg $N_{oxidized}^{-1}$
EAB (organic)	4.81 ± 1.31	71.30 ± 14.30	–	–	–
EAB (inorganic)	3.59 ± 1.21	23.59 ± 14.96	14.1 ± 4.5	0.266 ± 0.177	0.661 ± 0.403
AOB	1.00 ± 0.31	10.79 ± 2.04	5.9 ± 0.6	0.023 ± 0.012	0.049 ± 0.033
AOB2	1.14 ± 0.18	8.89 ± 1.45	6.9 ± 2.5	0.038 ± 0.019	0.052 ± 0.028
AnAOB	1.16 ± 0.46	1.65 ± 0.39	5.0 ± 0.5	0.022 ± 0.011	0.063 ± 0.047

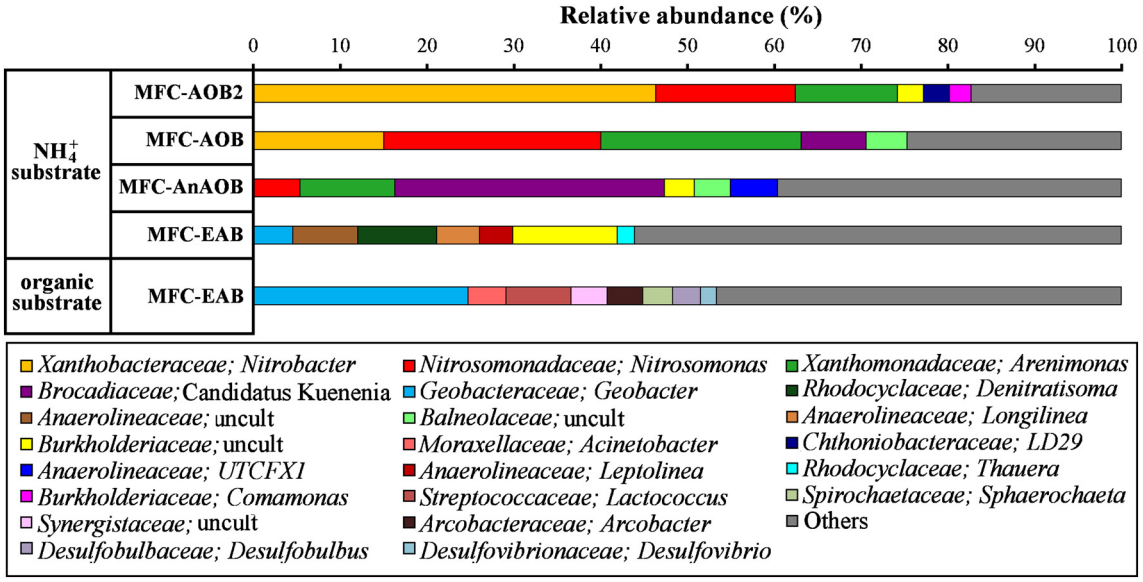

Fig. 5. Relative abundance of bacterial genera from the microbial communities sampled at the anode of MFC-EAB fed with organic and NH_4^+ substrates and MFC-AOB, MFC-AnAOB and MFC-AOB2. The relative abundance is defined as a percentage of the total microbial sequences in a sample. Genera that account for ≥3 % of at least one 16S rRNA gene sequence are shown, while genera with an abundance of <3 % in all sequences are grouped into Others.

increase in internal resistance from 10 Ω to 619 Ω when organic compounds were not available. The performance in our study was likely favoured by organic compounds adsorbed on the GAC combined with the organic compounds derived from the bacterial decay. These phenomena decreased the impact of organic matter absence during microbial community adaptation.

The coulombic efficiency reveals the system's ability to convert the chemical energy of an electron donor into electricity. Based on the results obtained in this study, the MFC-EAB reactor presented significantly higher ($p < 0.001$) CE (of 14.1 ± 4.5 %) compared to MFC-AOB (5.9 ± 0.6 %) and MFC-AnAOB (5.0 ± 0.5 %). In the MFC-EAB, non-electroactive ammonia-oxidizing bacteria were not found. Thus ammonia oxidation pathways that would have consumed nitrogen without generating current, such as aerobic nitrification and conventional anammox, were avoided.

The anode potential observed at open circuit mode was +261 ± 12 mV vs SHE. This potential is closer to the potential of +0.12 V vs SHE, from hydroxylamine (NH_2OH) oxidation by hydroxylamine oxidoreductase (HAO), than +0.48 V vs SHE, from NO_2^- oxidation by nitrite oxidoreductase (NXR) (Poughon et al., 2001).

The effluent of the anode chamber of MFC-EAB had only 7.7 ± 0.6 mg NO_3^--N L^{-1}. This NO_3^--N concentration level was significantly lower ($p < 0.001$) compared to that of MFC-AOB (32 ± 14.4 mg NO_3^--N L^{-1}) and MFC-AnAOB (33.8 ± 16.6 mg NO_3^--N L^{-1}). The known cytochrome system utilized by EAB, such as *Geobacter*, in EET is coupled with the formal redox potential of −0.28 V vs. SHE, when acetate is available (Joshi et al., 2021). Thus, the utilization of another electron source with higher redox potential means less amount of energy would be available for the growth of bacteria. The coupling of NO_2^- oxidation with EET would yield lower amount of energy in comparison to NH_2OH oxidation. This might have exceeded the energetic limit of respiration by EAB metabolism, configuring an unfeasible respiration pathway. This explains the accumulation of NO_2^- instead of NO_3^- in MFC-EAB.

So, the EET mechanism in MFC-EAB was likely associated with ammonia oxidation to NO_2^-. This explains the immediate NO_2^--N accumulation in the anode chamber effluent when organic carbon was not available and the significantly lower NO_3^--N concentration.

Geobacter was the only known EAB found in MFC-EAB (inorganic). However, an aerobic or anaerobic pathway of ammonia oxidation by *Geobacter* species is not supported by current knowledge on their enzymatic machinery. This suggests the current observed in MFC-EAB (inorganic) was generated by activity or interactions of bacteria not yet described as EAB.

The anode potentials of MFC-EAB at open circuit mode were lower than the values observed for MFC-AOB (Fig. 4c). This means reactions of the EET mechanism in MFC-EAB could deliver electrons at a higher potential energy level in comparison to MFC-AOB. In BES utilizing organic substrate, EAB can transfer electrons directly to the anode or utilizing a solid conductive matrix, avoiding electron shuttles. Thus, loss of energy by an EET step involving redox-active meditators is avoided by these mechanisms. So, the EET mechanism of EAB oxidizing ammonia in MFC-EAB is most likely center in mechanisms other than electron shuttles. This is also compatible with the higher CE of MFC-EAB.

In this sense, EET generated by a solid conductive matrix mechanism could have contributed to the higher power output observed for MFC-EAB. In this mechanism, bacteria can couple their outer membrane cytochromes with structures named nanowires, which relate to other sections of the biofilm and the anode. Hence, bacteria relying on this mechanism, such as *Geobacter*, are not limited by surface area to directly transfer electrons to the electrode or by diffusion of electron shuttles. This results in thicker biofilms and a higher maximum current rate in comparison with bacteria relying solely on EET by direct contact with electrode or electron shuttles (Torres et al., 2010). In this regard, the semi-conducive matrix produced by EAB with organic wastewater could have contributed to the current generation of MFC-EAB oxidizing NH_4^+. This is in accordance with the relatively stable internal resistance of MFC-EAB despite changes in the wastewater composition.

The ammonia oxidation in MFC-EAB is a process not yet described in the literature. This process is not catalyzed by AOB or AnAOB typically involved in nitrification and anammox and presents advantages: (i) biochemical reactions immediately start after organic carbon depletion; (ii) does not require aeration; (iii) the metabolic pathway favors NO_2^- production instead of NO_3^-. In terms of energy generation, the utilization of NH_4^+ represents an additional energy source within wastewater in comparison to conventional MFC and anaerobic digestion, which are dependent on organic substrates. The adaptation of EAB biofilm to potentially take part in the ammonia oxidation coupled to EET to the anode highlights the flexibility of MFC systems in terms of biotechnological applications. This ability may be explored for energy generation and quantified in the mass balance of the nitrogen cycle in ammonia and Fe (III) oxides rich environments.

3.4. Current generation by ammonia oxidizing bacteria

MFC-AOB harbored a predominance of *Nitrosomonas* (25 %), *Arenimonas* (23 %) and *Nitrobacter* (15 %). These bacteria were also found to be the most abundant genera in MFC-AOB2, though in different proportions: *Nitrobacter* (46.3 %), *Nitrosomonas* (16 %) and *Arenimonas* (11.7 %).

Nitrosomonas and *Nitrobacter* are autotrophic aerobic bacteria responsible for the conversion of NH_3 to NO_2^-, and NO_2^- to NO_3^-, respectively (Daims et al., 2016; Sharma and Ahlert, 1977). *Arenimonas* can use NO_3^- as an electron acceptor in heterotrophic, autotrophic or cathodic denitrification (Xing et al., 2018; Zhang et al., 2019a).

Based on the presence of *Nitrobacter* at considerable relative abundance, NO_3^- accumulation is expected. However, NO_2^- was the main oxidized nitrogen in the anode effluent. This indicates that NO_3^- expected to be produced by *Nitrobacter* could have been followed by further nitrogen reduction or assimilatory process (Han and Zhou, 2022; Kuypers et al., 2018).

Nitrosomonas activity is expected to produce NO_2^-. In this case, NO_3^- can be produced by *Nitrobacter* from NO_2^- oxidation and utilized as electron acceptor by *Arenimonas* in an incomplete denitrification process. This combination of reactions could have led to NO_2^- accumulation. Accumulation of NO_2^- has been reported with the presence of *Arenimonas* in simultaneous desulfurization and denitrification reactors (Zeng et al., 2018) and in single chamber BES (Zhang et al., 2019b).

The conventional oxidation mechanism by NOB is dependent of dissolved oxygen. This was particularly important in MFC-AOB2, in which oxygen diffused back from the cathode chamber through the internal hydraulic connection. This explains the higher proportion of *Nitrobacter* found in MFC-AOB2, which yielded a dissolved oxygen (DO) concentration of 1.73 ± 0.33 mg L^{-1}. The fact that the anammox bacteria *Candidatus* Kuenenia have been shown to be inhibited by dissolved oxygen (Kartal et al., 2011) and these bacteria were found in MFC-AOB (relative abundance of 7.4 %) but not in MFC-AOB2 is another indication that oxygen availability influenced microbial activity in MFC-AOB and MFC-AOB2. In this sense, conventional nitrification utilizing oxygen diffused from the cathode chamber could have been partially responsible for ammonia oxidation in our study.

So, to evaluate the influence of anaerobic conditions on MFC-AOB, this reactor was operated for 13 days with N_2 purging to avoid any accumulation of dissolved oxygen in the anode chamber. Low DO levels are expected to impose limitations on *Nitrosomonas* activity (Yu and Chandran, 2010), but the accumulation of NO_2^- was not affected by N_2 purging (Fig. S16). This finding differs from the findings presented by Hussain et al. (2016), who pointed out that oxygen is required to produce NO_2^- and NO_3^- in a MEC. The occurrence of ammonia oxidation with nitrite production in BES regardless of high oxygen levels is the key feature of BEAO.

This process may also be explored for other bioprocess applications not related to power output. For instance, the accumulation of NO_2^- is a promising approach to be combined with the conventional anammox process. This combination should result in nitrogen removal and is not dependent on organic carbon or aeration.

Some studies have shown that BEAO under anaerobic conditions resulted in the production of N_2 (Siegert and Tan, 2019; Vilajeliu-Pons et al., 2018). Alternatively, under low DO conditions, AOB can produce NO and N_2O (Chandran et al., 2011). The loss of dissolved nitrogen in this process may have also contributed to the relatively higher global nitrogen removal in the anode chamber of MFC-AOB (25 ± 13 %) compared to MFC-AOB2 (15 ± 12 %). Although N_2O production is commonly not desired in WWTP, since it is a greenhouse gas (296 times stronger than CO_2), it can also be used as a renewable energy source if properly captured (Lin et al., 2018).

The following sections discuss how current was generated in MFC-AOB and MFC-AOB2 as well as the role of oxygen in the molecular mechanism. Fig. 6a shows that the anode potential became more negative with N_2 purging, and the potential became more positive upon the cessation of N_2 purging. This observation implies that the absence of oxygen led to an improvement in the anode's performance. So, EET produced by the electroactive biofilm was adversely affected by the presence of oxygen.

Although the NOB *Nitrobacter* grew in the MFC-AOB and MFC-AOB2 reactors, they do not appear to be responsible for the EET. The presence of

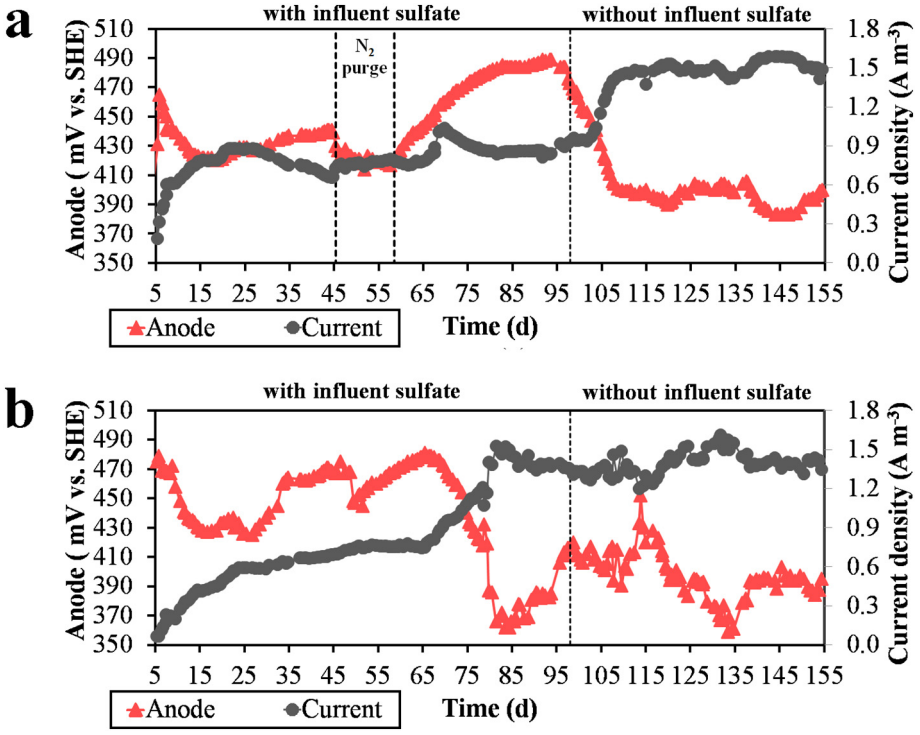

Fig. 6. Effect of (a) N_2 purging and sulfate availability in the anode chamber on the (△) anode potential and (●) current generation for MFC-AOB; and (b) sulfate availability in the influent on the anode potential (△) and current generation (●) for MFC-AnAOB.

NOB in BES has not been widely reported in the literature (Li et al., 2018; Lovley and Holmes, 2022). Furthermore, the NO_2^- oxidation potential (+0.48 V vs SHE) is higher than the anode OCPs observed when power output was stable (Fig. 3c). So, the electrons transferred to anode were released from a reaction with more negative redox potential than NO_2^- oxidation.

In addition, the utilization of an EET mechanism by NOB would result in considerable less energy in comparison to its conventional respiration mechanism. Normally, NO_2^- is oxidized to NO_3^- by NOB through the nitrite oxidoreductase (NXR), releasing two electrons to the respiratory chain. Then oxygen is utilized as the terminal electron acceptor in a reaction with redox potential of 0.82 V vs. SHE (Poughon et al., 2001; He and Angenent, 2006; Hemp et al., 2016). In our, study, oxygen availability was limited in the anode chamber. Due to energy losses related to activation of the oxygen reduction reaction on the cathode, a maximum open-circuit potential of 0.60 V vs. SHE, instead of 0.82 V vs. SHE, was observed for the cathode of MFC-AOB. Hence, by coupling the NXR with EET to the anode, NOB would obtain 65 % less energy compared with conventional respiration. Therefore, the lack of oxygen and energy losses associated with an EET-based respiration may have limited the growth and activity of NOB. This also explains the nitrite accumulation.The indirect contribution of AOB to the current generation based on the production of extracellular polymeric substances (EPS) as a source of electron donors for EET was considered elsewhere (He et al., 2009). However, the absence of heterotrophic EAB in the anodes of MFC-AOB and MFC-AO2 (Fig. 5) implies EPS was not a significant source of electrons. Alternatively, other bacteria present in these reactors whose EET ability has not yet been discovered may have contributed to the current generation.

This finding suggests that the power generation capacity of these reactors is related to EET through a pathway that has not yet been described, and which is possibly associated with a new EAB and/or AOB. We believe that the AOB were the primary bacteria involved in energy generation in MFC-AOB and MFC-AOB2. The MFC-AOB reactor, which exhibited a higher relative abundance of the AOB *Nitrosomonas*, presented a greater maximum power density compared to MFC-AOB2 (Fig. 4c). *Nitrosomonas* sp. have been shown to be predominant in the anodes of BES where ammonia is the electron donor (He et al., 2009; Qu et al., 2014; Vilajeliu-Pons et al., 2018; Zhan et al., 2014).

The generation of energy in MFC-AOB and MFC-AOB2 by AOB was likely through a pathway involving NH_2OH oxidation, which is compatible with the results of Vilajeliu-Pons et al. (2018). This is supported by the anode OCP of MFC-AOB (+0.38 V vs SHE in the last polarization curve). This potential is compatible with the NH_2OH oxidation potential of +0.12 V vs SHE, considering inevitable energy losses by the EET mechanism.

To transfer the electrons released from NH_2OH oxidation to the anode, anaerobic condition is required, since oxygen is used as a more efficient final electron acceptor (He et al., 2009). In this case, a different pathway is needd to support AOB growth without oxygen, which is discussed as follows.

It is worth noting that molecular oxygen plays a crucial role in the conversion of ammonia to hydroxylamine by the activity of ammonia monooxygenase (AMO) (Maalcke et al., 2014). In this regard, the necessity of oxygen in nitrifying BES should only be considered for hydroxylamine production, and not as the final electron acceptor. Hence, conventional nitrification may have contributed to the nitrite accumulation observed in this study, but in a BES the electrode replaces oxygen as the final electron acceptor in the EET process. This explains the observed current in MFC-AOB and MFC-AOB2.

AOB bacteria have not yet been proven capable of achieving EET by direct contact with a solid-state electron acceptor. It is known, though, that in conventional MFC, redox-active components produced by bacteria, including phenazine derivatives, quinones and flavins, can act as electron shuttles (Philips et al., 2016; Zhu et al., 2021). The electron shuttles are coupled to the respiratory chain, supporting the production of ATP. In a nitrifying MFC, they carry the electrons obtained by NH_4^+-N oxidation outside the bacteria to the surface of a solid electron acceptor. Then electron shuttles are oxidized on the anode and become available to carry more electrons. EET by electron shuttle is consistent with the findings of by Qu et al. (2014) in a MEC dominated by *Nitrosomonas*. In their study, current generation decreased when the medium was replaced and was immediately restored to 85 % of its original level when the filtered medium (0.22 μm-pore-diameter membrane) was returned to the anode chamber.

This mechanism may have been utilized by AOB to achieve EET here. In this regard, more energy would have been lost by an intermediate EET step in MFC-AOB compared to MFC-EAB, in which EET by direct contact and solid conductive matrix was considered plausible. This is in accordance with the lower potential energy level of the electrons delivered to the anode of MFC-AOB in comparison to MFC-EAB (Fig. 4c). More studies with pure culture of AOB are necessary to confirm the electron shuttle mechanism by these bacteria.

The results obtained for MFC-AOB showed BEAO is a feasible process and that elevated levels of DO are not strictly required. On the contrary, when oxygen accumulation was avoided, the EET improved. Considering our results, aeration in the anode chamber is not necessary to achieve BEAO. Thus, this novel process can lead to a technological breakthrough in terms of reducing the energy consumption of WWTPs. The implications of this in terms of energy savings are further discussed in the Section 3.6.

3.5. Current generation by anammox bacteria

Candidatus Kuenenia, an anammox representative, was the most abundant bacteria (31.1 %) found in MFC-AnAOB, followed by *Arenimonas* (10.9 %) and *Nitrosomonas* (5.3 %). The characteristics of the microbial community confirm anammox played a key role in the MFC-AnAOB reactor.

The MFC-AnAOB had an OCP of 319 ± 4 mV. This is significantly higher ($p < 0.001$) compared to MFC-AOB, which had an OCP of 216 ± 10 mV. The difference in the OCP values was caused by the anode potentials (Fig. 4c). Shaw et al. (2020) reported anode redox peaks in cyclic voltammetry with midpoint potentials of −0.01 ± 0.05 V vs. SHE for a BES with enrichment of anammox bacteria. This was lower than the potential of +0.73 ± 0.06 V vs. SHE obtained in another study where the BES was enriched with AOB (Vilajeliu-Pons et al., 2018). These results point to the difference between the reactions and the EET mechanism associated with the bioelectrochemical activity relating to AOB and AnAOB.

In anammox, bacteria obtain energy with the aid of hydrazine dehydrogenase (Hdh), which catalyzes the oxidation of N_2H_4. This reaction generates electrons at a redox potential of −0.75 V vs. SHE, which is lower than that of NH_2OH oxidation (+0.12 V vs. SHE) (Kartal et al., 2011; Li et al., 2018; Poughon et al., 2001). Thus, the coupling of EET with electrons released by Hdh is likely to result in a lower anode potential in relation to a mechanism associated with NH_2OH oxidation.

NH_2OH has been suggested as an intermediate for current generation from ammonia oxidation by anammox with N_2 being the final product (Shaw et al., 2020). However, NH_2OH oxidation does not solely explain the relatively lower reaction potentials obtained for AnAOB compared to those of AOB.

Considering the absence of oxygen, AOB in MFC-AnAOB may have conducted EET to the anode instead of using oxygen as the terminal electron acceptor. As previously discussed, the EET mechanism of AOB is coupled to a reaction with a higher redox potential than N_2H_4 oxidation. The mixed potential resulting from EET by both AOB (from NH_2OH oxidation) and AnAOB (from N_2H_4 oxidation) in MFC-AnAOB explains its anode OCPs being lower than the ones observed by MFC-AOB.

It is worth noting that the internal resistance of MFC-AnAOB was found to be at least 14-fold higher ($p \leq 0.045$) than that of the other reactors (Table S6). Also, the energy losses in MFC-AnAOB were mostly caused by the anode chamber instead of the cathode chamber (high anode internal resistance). This implies that the system was limited by the rate of EET to the anode, which is in accordance with the significantly lower ($p \leq 0.004$) CE obtained for the MFC-AnAOB reactor. Thus, despite the higher redox potential in the EET mechanism, a fewer amount of electrons was delivered to the anode by the bacterial community in the MFC-AnAOB.

In anammox, the electrons derived from N_2H_4 oxidation are transferred to the cytochrome *bc*1 complex. Subsequently, the electrons are redistributed to promote NO_2^- reduction to N_2 and N_2H_4 synthesis (Kartal et al., 2011). Thus, N_2H_4 could only be the source of electrons for EET through a different mechanism in which NO_2^- is not the electron acceptor.

NO_2^- oxidation to NO_3^- generates electrons for CO_2 fixation in traditional anammox. The reaction leads to the release of electrons at +0.43 V (Kartal et al., 2011). Therefore, NO_2^- does not seem to be the source of electrons for EET as the potential energy level of the electrons is incompatible with the observed anode potentials.

In this regard, Shaw et al. (2020) showed that when NO_2^- is available, current is not generated by a microbial community enriched with AnAOB. NO_2^- seems to be a preferable electron acceptor in comparison to the anode. Thus, when NO_2^- is available, electrons are lost to the conventional anammox pathway. In our study, part of the NO_2^--N found in the anode chamber was produced by AOB. In this case, AOB activity indirectly hampered EET through AnAOB.

3.6. Influence of SO_4^{2-} over current generation

In terms of SO_4^{2-} availability, there were no immediate changes in the MFC-AnAOB reactor's current generation (Fig. 6b). As a result, SO_4^{2-} have no effect on the dominant EET mechanism in MFC-AnAOB.

In contrast, for MFC-AOB, the results clearly show that influent SO_4^{2-} (551 ± 77 mg L^{-1}) exerted a negative effect on the performance of the bioanode (Fig. 6a). When SO_4^{2-} was not available, the anode potential of MFC-AOB immediately decreased from approximately +480 mV vs. SHE to less than +405 mV vs. SHE. The immediate changes observed for MFC-AOB suggest SO_4^{2-} directly affected the EET.

Sulfur species have been regarded as mediators, favoring the current generation in BES fed with organic matter but its role in the BEAO is not elucidated (Philips et al., 2016). Sulfate-reducing microorganisms (SRM) use SO_4^{2-} as the terminal electron acceptor for the oxidation of various organic compounds (Zhao et al., 2020). Considering the absence of organic carbon, sulfate-reducing ammonium oxidation (sulfammox) may have played a role in ammonia oxidation. In this process, bacteria, such as *Brocadia Anammoxoglobus Sulfate* and *Bacillus Benzoevorans*, utilize NH_4^+ as an electron donor and SO_4^{2-} as the electron acceptor, generating S^0 and N_2 (or HS^- and NO_2^- as intermediates) (Dominika et al., 2021).

Alternatively, SRM have a mechanism to directly collect electrons from the electrode to accomplish SO_4^{2-} reduction (Agostino and Rosenbaum, 2018). Also, SRM can achieve interspecies electrons transfer with anaerobic methane oxidizing Archaea via sulfur compounds as mediators (Shrestha and Rotaru, 2014). Likewise, a direct or indirect interspecies electrons transfer mechanism between AOB and SRM could have been responsible for the results observed for MFC-AOB. The occurrence of sulfammox or interspecies electron transfer culminates in fewer electrons available for EET to the anode.

In this regard, stoichiometric theoretical consumption ratio of sulfammox process is 2:1 (NH_4^+:SO_4^{2-}), which represents 0.37 g NH_4^+/g SO_4^{2-} (Dominika et al., 2021). In our study, an influent g NH_4^+/g SO_4^{2-} ratio of 1.2 ± 0.5 was applied. In this condition, sulfammox bacteria could have consumed up to 30 % of the electrons released by NH_2OH oxidation.

Thus, by ceasing electron loss by sulfammox, a 1.45 fold increase in current generation should be expected. The results of MFC-AOB showed that current density was 0.89 ± 0.05 A m^{-3} when SO_4^{2-} was available and rapidly increased to 1.26 ± 0.2 A m^{-3} in the first 15 d when SO_4^{2-} was not available (Fig. 6a). This represents 1.4 fold more current, which was followed by a CE increase from 4.0 ± 1.0 % to 5.9 ± 0.6 %. Moreover, in many occasions total nitrogen removal was followed by SO_4^{2-} removal (see Figs. S24–S26). These results demonstrate that in a nitrifying MFC dominated by AOB sulfate can limit current generation rather than favoring EET.

In wastewaters with a high concentration of readily biodegradable COD, such as vinasse, simultaneous removal of organic matter and SO_4^{2-} by SRM is expected in the initial stages of the biological treatment (Barrera et al., 2014). In this case, SO_4^{2-} should not interfere with NH_4^+ oxidation in the following stages of treatment. However, SO_4^{2-} may not be efficiently removed from wastewater with COD:SO_4^{2-} ratio lower than 0.65 or with high proportion of recalcitrant organic matter, such as landfill leachate and some industrial streams (Lens et al., 1998). In this case, SO_4^{2-} will persist in the wastewater at high concentrations and hinder the current generation from BEAO by AOB.

The main pathways proposed in this study for MFC-EAB, MFC-AOB and MFC-AnAOB are graphically presented in Figs. S7–S9.

3.7. Projected energy savings by BEAO

The maximum power densities achieved by MFC-EAB and MFC-AOB were similar or even higher than the ones reported in the literature for MFCs with GAC electrodes utilizing organic compounds as electron donors (Table S7). This demonstrates the MFC configuration and operation in our study is compatible with relatively high power output. In terms of NH_4^+ removal, rates achieved in this study (0.066 to 0.093 g L^{-1} d^{-1}) based on the oxidized ammonia (excluding the ammonium migration to the cathode) are in the overall range reported in literature regarding ammonia oxidation in BES (Hussain et al., 2016; Kim et al., 2016; Koffi and Okabe, 2021; Pous et al., 2021; Vilajeliu-Pons et al., 2018; Yin et al., 2015; Zhan et al., 2012; Zhu et al., 2021, Table S8). However, the biomass concentrations and microbial diversity in the previous studies could have been very well different than in our study. Therefore, we suggest that such direct comparison of results may not always be possible.

In comparison to conventional nitrification systems, our results revealed that the energy from BEAO by MFC-EAB, MFC-AOB, MFC-AOB2 and MFC-AnAOB can reduce the electricity consumption for nitrogen oxidation in, respectively, 59 %, 44 %, 31 %, and 7 %. A R_{ext} of 300 Ω was applied in all reactors while the internal resistances of MFC-EAB, MFC-AOB, MFC-AOB2 and MFC-AnAOB were, respectively, 19.5 Ω, 18.9 Ω, 20.9 Ω and 299.3 Ω. Thus, apart from the MFC-AnAOB, the cathodophilic (details in Section 8 of SM) and anodophilic activity (and energy savings, consequently) could potentially be further increased by adjusting the external resistance to equal the internal resistance (Koók et al., 2021). Hence higher coulombic efficiencies and power outputs are expected by optimizing the R_{ext}.

Considering the maximum power output obtained in the polarization curve right after starting the NH_4^+ substrate feeding and achieving stable NH_4^+ oxidation, MFC-EAB showed a remarkable performance of 4.02 kWh per kg of oxidized NH_4^+-N. This rate is 4.7 fold higher than the energy necessary for artificial aeration in a nitrification process. This outcome highlights the potential application of the process to reduce the energy consumption in WWTPs. Therefore, technological and operational strategies combining the simultaneous or alternated organic matter and NH_4 oxidation in MFC should be further explored.

4. Conclusions

Electricity-generating bioelectrochemical ammonium oxidation by biofilms enriched with EAB, AOB, and AnAOB were compared in continuously operated MFCs. All MFCs presented comparable ammonia oxidation rates (between 0.066 and 0.083 g NH_4^+-N L^{-1} d^{-1}) with nitrite as the main final product. However, diverse energy generation levels were observed by each group. The power output of the biofilm enriched with AnAOB was limited by a substantial higher energy loss related to the anode. This resulted in maximum power density of 0.2 W m^{-3}, which limits practical energy-generating applications. The AOB enriched biofilm achieved maximum power density up to 1.44 W m^{-3}, representing between 31 % and 44 % less electricity consumption compared to conventional nitrification. Additionally, AOB's EET pathway was found to be adversely affected by oxygen and sulfate presence. Significantly, the biofilm previously enriched with EAB fed with organic carbon quickly adapted to oxidize ammonia when organic matter was not supplied. Despite from the decrease of heterotrophic EAB in the microbial community, internal

resistance did not substantially change and the most elevated power densities, between 1.38 and 11 W m^{-3}, were achieved. Compared to conventional nitrification, projected energy savings (based on lab-scale experiment) by the EAB enriched biofilm ranged from 475 %, after 23 days without organic carbon supply, to 59 %, after 83 days. Hence, the ability of the MFC system to shift from oxidation of organic carbon to ammonia nitrogen, while temporally preserving relatively high power output, may be explored in novel applications. Based on these results, we showed for the first time that complex microbial interactions in MFCs can lead to N routes not reported in the N cycle, which creates new possibilities for sustainable wastewater treatment.

CRediT authorship contribution statement

Vitor Cano: Conceptualization, Methodology, Formal analysis, Investigation, Writing – original draft, Project administration, Visualization. **Marcelo A. Nolasco:** Conceptualization, Methodology, Formal analysis, Investigation, Writing – original draft, Project administration, Visualization. **Halil Kurt:** Formal analysis, Writing – review & editing, Supervision. **Chenghua Long:** Investigation, Formal analysis, Writing – review & editing. **Julio Cano:** Investigation. **Sabrina C. Nunes:** Investigation. **Kartik Chandran:** Resources, Writing – review & editing, Supervision, Project administration, Funding acquisition.

Data availability

Data utilized in the study is available in the supplementary information or publicly available at NCBI (BioProject ID: PRJNA803873).

Declaration of competing interest

The authors declare that they have no known competing financial interests or personal relationships that could have appeared to influence the work reported in this paper.

Acknowledgments

This work was supported by FAPESP [Process number: 17/24524-0, 17/10325-5 and 19/06266-9], Coordenação de Aperfeiçoamento de Pessoal de Nível Superior - Brazil (CAPES) [Finance Code 001] and National Science Foundation [project CBET 1706726]. The authors would like to thank for the English grammatical review provided by Beria Hatice Hos. The authors are grateful to Dr. Catherine Hoar and Dr. Minxi Jiang for providing the nitrifying and anammox biomass utilized in this study.

Appendix A. Supplementary data

Supplementary data to this article can be found online at https://doi.org/10.1016/j.scitotenv.2023.161688.

References

Agostino, V., Rosenbaum, M.A., 2018. Sulfate-reducing ElectroAutotrophs and their applications in bioelectrochemical systems. Front. Energy Res. 6, 55. https://doi.org/10.3389/fenrg.2018.00055.

Anastas, P., Nolasco, M., Kerton, F., Kirchhoff, M., Licence, P., Pradeep, T., Subramaniam, B., Moores, A., 2021. The power of the United Nations sustainable development goals in sustainable chemistry and engineering research. ACS Sustainable Chem. Eng. 9, 8015–8017. https://doi.org/10.1021/acssuschemeng.1c03762.

APHA, 2017. Standard Methods for the Examination of Water and Wastewater. 23rd edition. American Public Health Association, Washington, DC.

Barbosa, S.G., Peixoto, L., Soares, O.S.G.P., Pereira, M.F.R., Heijne, A.T., Kuntke, P., Alves, M.M., Pereira, M.A., 2018. Influence of carbon anode properties on performance and microbiome of microbial electrolysis cells operated on urine. Electrochim. Acta 267, 122–132. https://doi.org/10.1016/j.electacta.2018.02.083.

Barrera, E.L., Spanjers, H., Romero, O., Rosa, E., Dewulf, J., 2014. Characterization of the sulfate reduction process in the anaerobic digestion of a very high strength and sulfate rich vinasse. Chem. Eng. J. 248, 383–393. https://doi.org/10.1016/j.cej.2014.03.057.

Brotto, A.C., Annavajhala, M.K., Chandran, K., 2018. Metatranscriptomic investigation of adaptation in NO and N2O production from a lab-scale nitrification process upon repeated exposure to anoxic-aerobic cycling. Front. Microbiol. 9. https://doi.org/10.3389/fmicb.2018.03012.

Caizán-Juanarena, L., Sleutels, T., Borsje, C., ter Heijne, A., 2020. Considerations for application of granular activated carbon as capacitive bioanode in bioelectrochemical systems. Renew. Energy 157, 782–792. https://doi.org/10.1016/j.renene.2020.05.049.

Cano, V., 2020. Energy generation in a novel microbial fuel cell: characterization and dynamics of microbial communities using organic matter and ammonia as electron donors (PhD in Sustainability). University of Sao Paulo, São Paulo https://doi.org/10.11606/T.100.2020.tde-19052020-101339.

Cano, V., Vich, D.V., Rousseau, D.P.L., Lens, P.N.L., Nolasco, M.A., 2019. Influence of recirculation over COD and N-NH4 removals from landfill leachate by horizontal flow constructed treatment wetland. Int. J. Phytorem. 21, 998–1004. https://doi.org/10.1080/15226514.2019.1594681.

Cano, V., Vich, D.V., Andrade, H.H.B., Salinas, D.T.P., Nolasco, M.A., 2020. Nitrification in multistage horizontal flow treatment wetlands for landfill leachate treatment. Sci. Total Environ. 704, 135376. https://doi.org/10.1016/j.scitotenv.2019.135376.

Cano, V., Cano, J., Nunes, S.C., Nolasco, M.A., 2021. Electricity generation influenced by nitrogen transformations in a microbial fuel cell: assessment of temperature and external resistance. Renew. Sust. Energ. Rev. 139, 110590. https://doi.org/10.1016/j.rser.2020.110590.

Cao, Y., van Loosdrecht, M.C.M., Daigger, G.T., 2017. Mainstream partial nitritation-anammox in municipal wastewater treatment: status, bottlenecks, and further studies. Appl. Microbiol. Biotechnol. 101, 1365–1383. https://doi.org/10.1007/s00253-016-8058-7.

Chandran, K., Smets, B.F., 2000. Single-step nitrification models erroneously describe batch ammonia oxidation profiles when nitrite oxidation becomes rate limiting. Biotechnol. Bioeng. 68, 396–406. https://doi.org/10.1002/(SICI)1097-0290(20000520)68:4<396::AID-BIT5>3.0.CO;2-S.

Chandran, K., Stein, L.Y., Klotz, M.G., van Loosdrecht, M.C.M., 2011. Nitrous oxide production by lithotrophic ammonia-oxidizing bacteria and implications for engineered nitrogen-removal systems. Biochem. Soc. Trans. 39, 1832–1837. https://doi.org/10.1042/BST20110717.

Chen, H., Zheng, P., Zhang, J., Xie, Z., Ji, J., Ghulam, A., 2014. Substrates and pathway of electricity generation in a nitrification-based microbial fuel cell. Bioresour. Technol. 161, 208–214. https://doi.org/10.1016/j.biortech.2014.02.081.

Chen, H., Liu, K., Yang, E., Chen, J., Gu, Y., Wu, S., Yang, M., Wang, H., Wang, D., Li, H., 2023. A critical review on microbial ecology in the novel biological nitrogen removal process: dynamic balance of complex functional microbes for nitrogen removal. Sci. Total Environ. 857, 159462. https://doi.org/10.1016/j.scitotenv.2022.159462.

Chrispim, M.C., Scholz, M., Nolasco, M.A., 2020. A framework for resource recovery from wastewater treatment plants in megacities of developing countries. Environ. Res. 188, 109745. https://doi.org/10.1016/j.envres.2020.109745.

Colacicco, A., Zacchei, E., 2020. Optimization of energy consumptions of oxidation tanks in urban wastewater treatment plants with solar photovoltaic systems. J. Environ. Manag. 276, 111353. https://doi.org/10.1016/j.jenvman.2020.111353.

Daims, H., Lücker, S., Wagner, M., 2016. A new perspective on microbes formerly known as nitrite-oxidizing bacteria. Trends Microbiol. 24, 699–712. https://doi.org/10.1016/j.tim.2016.05.004.

Dominika, G., Joanna, M., Jacek, M., 2021. Sulfate reducing ammonium oxidation (SULFAMMOX) process under anaerobic conditions. Environ. Technol. Innov. 22, 101416. https://doi.org/10.1016/j.eti.2021.101416.

Drewnowski, J., Remiszewska-Skwarek, A., Duda, S., Łagód, G., 2019. Aeration process in bioreactors as the main energy consumer in a wastewater treatment plant. Review of solutions and methods of process optimization. Processes 7, 311. https://doi.org/10.3390/pr7050311.

Engelberth, A.S., Niu, W., Ventura, S.P.M., Nair, S., Nolasco, M.A., Carrier, D.J., 2021. ACS sustainable chemistry & engineering welcomes manuscripts on alternative feedstocks. ACS Sustainable Chem. Eng. 9, 4702–4703. https://doi.org/10.1021/acssuschemeng.1c01929.

España-Gamboa, E., Mijangos-Cortes, J., Barahona-Perez, L., Dominguez-Maldonado, J., Hernández-Zarate, G., Alzate-Gaviria, L., 2011. Vinasses: characterization and treatments. Waste Manag. Res. 29, 1235–1250. https://doi.org/10.1177/0734242X10387313.

Fedorovich, V., Knighton, M.C., Pagaling, E., Ward, F.B., Free, A., Goryanin, I., 2009. Novel electrochemically active bacterium phylogenetically related to Arcobacter butzleri, isolated from a microbial fuel cell. Appl. Environ. Microbiol. https://doi.org/10.1128/AEM.01345-09.

Gu, Y., Li, Y., Li, X., Luo, P., Wang, H., Robinson, Z.P., Wang, X., Wu, J., Li, F., 2017. The feasibility and challenges of energy self-sufficient wastewater treatment plants. Appl. Energy 204, 1463–1475. https://doi.org/10.1016/j.apenergy.2017.02.069.

Gude, V.G., 2015. Energy and water autarky of wastewater treatment and power generation systems. Renew. Sust. Energ. Rev. 45, 52–68. https://doi.org/10.1016/j.rser.2015.01.055.

Han, F., Zhou, W., 2022. Nitrogen recovery from wastewater by microbial assimilation – a review. Bioresour. Technol. 363, 127933. https://doi.org/10.1016/j.biortech.2022.127933.

Hassan, M., Wei, H., Qiu, H., Su, Y., Jaafry, S.W.H., Zhan, L., Xie, B., 2018. Power generation and pollutants removal from landfill leachate in microbial fuel cell: variation and influence of anodic microbiomes. Bioresour. Technol. 247, 434–442. https://doi.org/10.1016/j.biortech.2017.09.124.

He, Z., Angenent, L.T., 2006. Application of bacterial biocathodes in microbial fuel cells. Electroanalysis 18, 2009–2015. https://doi.org/10.1002/elan.200603628.

He, Z., Kan, J., Wang, Y., Huang, Y., Mansfeld, F., Nealson, K.H., 2009. Electricity production coupled to ammonium in a microbial fuel cell. Environ. Sci. Technol. 43, 3391–3397. https://doi.org/10.1021/es803492c.

Hemp, J., Lücker, S., Schott, J., Pace, L.A., Johnson, J.E., Schink, B., Daims, H., Fischer, W.W., 2016. Genomics of a phototrophic nitrite oxidizer: insights into the evolution of photosynthesis and nitrification. ISME J. 10, 2669–2678. https://doi.org/10.1038/ismej.2016.56.

Hodgson, D.M., Smith, A., Dahale, S., Stratford, J.P., Li, J.V., Grüning, A., Bushell, M.E., Marchesi, J.R., Avignone Rossa, C., 2016. Segregation of the anodic microbial communities in a microbial fuel cell Cascade. Front. Microbiol. 7. https://doi.org/10.3389/fmicb.2016.00699.

Hussain, A., Manuel, M., Tartakovsky, B., 2016. A comparison of simultaneous organic carbon and nitrogen removal in microbial fuel cells and microbial electrolysis cells. J. Environ. Manag. 173, 23–33. https://doi.org/10.1016/j.jenvman.2016.02.025.

Jadhav, D.A., Ghangrekar, M.M., 2015. Effective ammonium removal by anaerobic oxidation in microbial fuel cells. Environ. Technol. 36, 767–775. https://doi.org/10.1080/09593330.2014.960481.

Johnson, D.B., Schideman, L.C., Canam, T., Hudson, R.J.M., 2018. Pilot-scale demonstration of efficient ammonia removal from a high-strength municipal wastewater treatment sidestream by algal-bacterial biofilms affixed to rotating contactors. Algal Res. 34, 143–153. https://doi.org/10.1016/j.algal.2018.07.009.

Joicy, A., Song, Y.-C., Lee, C.-Y., 2019. Electroactive microorganisms enriched from activated sludge remove nitrogen in bioelectrochemical reactor. J. Environ. Manag. 233, 249–257. https://doi.org/10.1016/j.jenvman.2018.12.037.

Joshi, K., Chan, C.H., Bond, D.R., 2021. Geobacter sulfurreducens inner membrane cytochrome CbcBA controls electron transfer and growth yield near the energetic limit of respiration. Mol. Microbiol. 116, 1124–1139. https://doi.org/10.1111/mmi.14801.

Kartal, B., Keltjens, J.T., Jetten, M.S.M., 2011. Metabolism and genomics of anammox bacteria. Nitrification. John Wiley & Sons, Ltd, pp. 179–200 https://doi.org/10.1128/9781555817145.ch8.

Kim, T., An, J., Lee, H., Jang, J.K., Chang, I.S., 2016. pH-dependent ammonia removal pathways in microbial fuel cell system. Bioresour. Technol. 215, 290–295. https://doi.org/10.1016/j.biortech.2016.03.167.

Kim, S.Y., Garcia, H.A., Lopez-Vazquez, C.M., Milligan, C., Herrera, A., Matosic, M., Curko, J., Brdjanovic, D., 2020. Oxygen transfer performance of a supersaturated oxygen aeration system (SDOX) evaluated at high biomass concentrations. Process Saf. Environ. Prot. 139, 171–181. https://doi.org/10.1016/j.psep.2020.03.026.

Koffi, N.J., Okabe, S., 2021. Bioelectrochemical anoxic ammonium nitrogen removal by an MFC driven single chamber microbial electrolysis cell. Chemosphere 274, 129715. https://doi.org/10.1016/j.chemosphere.2021.129715.

Koók, L., Nemestóthy, N., Bélafi-Bakó, K., Bakonyi, P., 2021. The influential role of external electrical load in microbial fuel cells and related improvement strategies: a review. Bioelectrochemistry 140, 107749. https://doi.org/10.1016/j.bioelechem.2021.107749.

Kuypers, M.M.M., Marchant, H.K., Kartal, B., 2018. The microbial nitrogen-cycling network. Nat. Rev. Microbiol. 16, 263–276. https://doi.org/10.1038/nrmicro.2018.9.

Lam, P., Kuypers, M.M.M., 2011. Microbial nitrogen cycling processes in oxygen minimum zones. Annu. Rev. Mar. Sci. 3, 317–345. https://doi.org/10.1146/annurev-marine-120709-142814.

Lee, J., Jeong, S., Long, C., Chandran, K., 2022. Size dependent impacts of a model microplastic on nitrification induced by interaction with nitrifying bacteria. J. Hazard. Mater. 424, 127363. https://doi.org/10.1016/j.jhazmat.2021.127363.

Lens, P.N.L., Visser, A., Janssen, A.J.H., Pol, L.W.H., Lettinga, G., 1998. Biotechnological treatment of sulfate-rich wastewaters. Crit. Rev. Environ. Sci. Technol. 28, 41–88. https://doi.org/10.1080/10643389891254160.

Leong, J.X., Daud, W.R.W., Ghasemi, M., Liew, K.B., Ismail, M., 2013. Ion exchange membranes as separators in microbial fuel cells for bioenergy conversion: a comprehensive review. Renew. Sust. Energ. Rev. 28, 575–587. https://doi.org/10.1016/j.rser.2013.08.052.

Li, M., Zhou, M., Tian, X., Tan, C., McDaniel, C.T., Hassett, D.J., Gu, T., 2018. Microbial fuel cell (MFC) power performance improvement through enhanced microbial electrogenicity. Biotechnol. Adv. 36, 1316–1327. https://doi.org/10.1016/j.biotechadv.2018.04.010.

Lin, Z., Sun, D., Dang, Y., Holmes, D.E., 2018. Significant enhancement of nitrous oxide energy yields from wastewater achieved by bioaugmentation with a recombinant strain of Pseudomonas aeruginosa. Sci. Rep. 8, 11916. https://doi.org/10.1038/s41598-018-30326-8.

Logan, B.E., 2012. Essential data and techniques for conducting microbial fuel cell and other types of bioelectrochemical system experiments. ChemSusChem 5, 988–994. https://doi.org/10.1002/cssc.201100604.

Lovley, D.R., Holmes, D.E., 2022. Electromicrobiology: the ecophysiology of phylogenetically diverse electroactive microorganisms. Nat. Rev. Microbiol. 20, 5–19. https://doi.org/10.1038/s41579-021-00597-6.

Ma, Y., Sundar, S., Park, H., Chandran, K., 2015. The effect of inorganic carbon on microbial interactions in a biofilm nitritation–anammox process. Water Res. 70, 246–254. https://doi.org/10.1016/j.watres.2014.12.006.

Maalcke, W.J., Dietl, A., Marritt, S.J., Butt, J.N., Jetten, M.S.M., Keltjens, J.T., Barends, T.R.M., Kartal, B., 2014. Structural basis of biological NO generation by octaheme oxidoreductases. J. Biol. Chem. 289, 1228–1242. https://doi.org/10.1074/jbc.M113.525147.

Nancharaiah, Y.V., Venkata Mohan, S., Lens, P.N.L., 2016. Recent advances in nutrient removal and recovery in biological and bioelectrochemical systems. Bioresour. Technol. 215, 173–185. https://doi.org/10.1016/j.biortech.2016.03.129.

Nolasco, M.A., Cano, V., Cano, J., 2022. Sistema bioeletroquímico sequencial empilhável para geração. de eletricidade BR102021005323A2.

Obata, O., Salar-Garcia, M.J., Greenman, J., Kurt, H., Chandran, K., Ieropoulos, I., 2020. Development of efficient electroactive biofilm in urine-fed microbial fuel cell cascades for bioelectricity generation. J. Environ. Manag. 258, 109992. https://doi.org/10.1016/j.jenvman.2019.109992.

Oksuz, S.T., Beyenal, H., 2021. Enhanced bioelectrochemical nitrogen removal in flow through electrodes. Sustainable Energy Technol. Assess. 47, 101507. https://doi.org/10.1016/j.seta.2021.101507.

Paquete, C.M., Rosenbaum, M.A., Bañeras, L., Rotaru, A.-E., Puig, S., 2022. Let's chat: communication between electroactive microorganisms. Bioresour. Technol. 347, 126705. https://doi.org/10.1016/j.biortech.2022.126705.

Philips, J., Verbeeck, K., Rabaey, K., Arends, J.B.A., 2016. 3 - electron transfer mechanisms in biofilms. In: Scott, K., Yu, E.H. (Eds.), Microbial Electrochemical and Fuel Cells. Woodhead Publishing, Boston, pp. 67–113 https://doi.org/10.1016/B978-1-78242-375-1.00003-4.

Poughon, L., Dussap, C.-G., Gros, J.-B., 2001. Energy model and metabolic flux analysis for autotrophic nitrifiers. Biotechnol. Bioeng. 72, 416–433. https://doi.org/10.1002/1097-0290(20000220)72:4<416::AID-BIT1004>3.0.CO;2-D.

Pous, N., Korth, B., Osset-Álvarez, M., Balaguer, M.D., Harnisch, F., Puig, S., 2021. Electrifying biotrickling filters for the treatment of aquaponics wastewater. Bioresour. Technol. 319, 124221. https://doi.org/10.1016/j.biortech.2020.124221.

Qu, B., Fan, B., Zhu, S., Zheng, Y., 2014. Anaerobic ammonium oxidation with an anode as the electron acceptor: anaerobic ammonium oxidation with electrode reduction. Environ. Microbiol. Rep. 6, 100–105. https://doi.org/10.1111/1758-2229.12113.

Ruiz-Urigüen, M., Steingart, D., Jaffé, P.R., 2019. Oxidation of ammonium by Feammox Acidimicrobiaceae sp. A6 in anaerobic microbial electrolysis cells. Environ. Sci.: Water Res. Technol. 5, 1582–1592. https://doi.org/10.1039/C9EW00366E.

Sayavedra-Soto, L.A., Arp, D.J., 2014. Ammonia-oxidizing bacteria: their biochemistry and molecular biology. Nitrification. John Wiley & Sons, Ltd, pp. 9–37 https://doi.org/10.1128/9781555817145.ch2.

Sharma, B., Ahlert, R.C., 1977. Nitrification and nitrogen removal. Water Res. 11, 897–925. https://doi.org/10.1016/0043-1354(77)90078-1.

Shaw, D.R., Ali, M., Katuri, K.P., Gralnick, J.A., Reimann, J., Mesman, R., van Niftrik, L., Jetten, M.S.M., Saikaly, P.E., 2020. Extracellular electron transfer-dependent anaerobic oxidation of ammonium by anammox bacteria. Nat. Commun. 11, 2058. https://doi.org/10.1038/s41467-020-16016-y.

Shrestha, P.M., Rotaru, A.-E., 2014. Plugging in or going wireless: strategies for interspecies electron transfer. Front. Microbiol. 5, 237. https://doi.org/10.3389/fmicb.2014.00237.

Siegert, M., Tan, A., 2019. Electric stimulation of ammonotrophic methanogenesis. Front. Energy Res. 7, 17. https://doi.org/10.3389/fenrg.2019.00017.

Strous, M., Kuenen, J.G., Jetten, M.S.M., 1999. Key physiology of anaerobic ammonium oxidation. Appl. Environ. Microbiol. 65, 3248–3250. https://doi.org/10.1128/AEM.65.7.3248-3250.1999.

Tang, J., Chen, S., Huang, L., Zhong, X., Yang, G., Zhou, S., 2017. Acceleration of electroactive anammox (electroammox) start-up by switching acetate pre-acclimated biofilms to electroammox biofilms. Bioresour. Technol. 243, 1257–1261. https://doi.org/10.1016/j.biortech.2017.08.033.

Torres, C.I., Marcus, A.K., Lee, H.-S., Parameswaran, P., Krajmalnik-Brown, R., Rittmann, B.E., 2010. A kinetic perspective on extracellular electron transfer by anode-respiring bacteria. FEMS Microbiol. Rev. 34, 3–17. https://doi.org/10.1111/j.1574-6976.2009.00191.x.

Vashi, H., Iorhemen, O.T., Tay, J.H., 2019. Extensive studies on the treatment of pulp mill wastewater using aerobic granular sludge (AGS) technology. Chem. Eng. J. 359, 1175–1194. https://doi.org/10.1016/j.cej.2018.11.060.

Vilajeliu-Pons, A., Koch, C., Balaguer, M.D., Colprim, J., Harnisch, F., Puig, S., 2018. Microbial electricity driven anoxic ammonium removal. Water Res. 130, 168–175. https://doi.org/10.1016/j.watres.2017.11.059.

Wang, D., Li, T., Huang, K., He, X., Zhang, X.-X., 2019. Roles and correlations of functional bacteria and genes in the start-up of simultaneous anammox and denitrification system for enhanced nitrogen removal. Sci. Total Environ. 655, 1355–1363. https://doi.org/10.1016/j.scitotenv.2018.11.321.

Whittaker, M., Bergmann, D., Arciero, D., Hooper, A.B., 2000. Electron transfer during the oxidation of ammonia by the chemolithotrophic bacterium Nitrosomonas europaea. Biochim. Biophys. Acta Bioenerg. 1459, 346–355. https://doi.org/10.1016/S0005-2728(00)00171-7.

Xing, W., Li, J., Li, D., Hu, J., Deng, S., Cui, Y., Yao, H., 2018. Stable-isotope probing reveals the activity and function of autotrophic and heterotrophic denitrifiers in nitrate removal from organic-limited wastewater. Environ. Sci. Technol. 52, 7867–7875. https://doi.org/10.1021/acs.est.8b01993.

Xu, S., Zhu, J., Meng, Z., Li, W., Ren, S., Wang, T., 2019. Hydrogen and methane production by co-digesting liquid swine manure and brewery wastewater in a two-phase system. Bioresour. Technol. 293, 122041. https://doi.org/10.1016/j.biortech.2019.122041.

Yin, X., Qiao, S., Zhou, J., Quan, X., 2015. Using three-bio-electrode reactor to enhance the activity of anammox biomass. Bioresour. Technol. 196, 376–382. https://doi.org/10.1016/j.biortech.2015.07.096.

Yu, R., Chandran, K., 2010. Strategies of Nitrosomonas europaea 19718 to counter low dissolved oxygen and high nitrite concentrations. BMC Microbiol. 10, 70. https://doi.org/10.1186/1471-2180-10-70.

Yüzbaşıoğlu, A.E., Avşar, C., Gezerman, A.O., 2022. The current situation in the use of ammonia as a sustainable energy source and its industrial potential. Curr. Res. Green Sustain. Chem. 5, 100307. https://doi.org/10.1016/j.crgsc.2022.100307.

Zekker, I., Rikmann, E., Tenno, Toomas, Menert, A., Lemmiksoo, V., Saluste, A., Tenno, Taavo, Tomingas, M., 2011. Modification of nitrifying biofilm into nitritating one by combination of increased free ammonia concentrations, lowered HRT and dissolved oxygen concentration. J. Environ. Sci. 23, 1113–1121. https://doi.org/10.1016/S1001-0742(10)60523-2.

Zekker, I., Rikmann, E., Tenno, Toomas, Seiman, A., Loorits, L., Kroon, K., Tomingas, M., Vabamäe, P., Tenno, Taavo, 2014. Nitritating-anammox biomass tolerant to high dissolved oxygen concentration and C/N ratio in treatment of yeast factory wastewater. Environ. Technol. 35, 1565–1576. https://doi.org/10.1080/09593330.2013.874492.

Zekker, I., Raudkivi, M., Artemchuk, O., Rikmann, E., Priks, H., Jaagura, M., Tenno, T., 2021. Mainstream-sidestream wastewater switching promotes anammox nitrogen removal rate in organic-rich, low-temperature streams. Environ. Technol. 42, 3073–3082. https://doi.org/10.1080/09593330.2020.1721566.

Zeng, Y., Zhou, J., Yan, Z., Zhang, X., Tu, W., Li, N., Tang, M., Yuan, Y., Li, X., Cao, Q., Huang, Y., 2018. The study of simultaneous desulfurization and denitrification process based on

the key parameters. Process Biochem. 70, 144–152. https://doi.org/10.1016/j.procbio.2018.04.007.
Zhan, G., Zhang, L., Li, D., Su, W., Tao, Y., Qian, J., 2012. Autotrophic nitrogen removal from ammonium at low applied voltage in a single-compartment microbial electrolysis cell. Bioresour. Technol. 116, 271–277. https://doi.org/10.1016/j.biortech.2012.02.131.
Zhan, G., Zhang, L., Tao, Y., Wang, Y., Zhu, X., Li, D., 2014. Anodic ammonia oxidation to nitrogen gas catalyzed by mixed biofilms in bioelectrochemical systems. Electrochim. Acta 135, 345–350. https://doi.org/10.1016/j.electacta.2014.05.037.
Zhang, Y., Zhao, Q., Jiang, J., Wang, K., Wei, L., Ding, J., Yu, H., 2017. Acceleration of organic removal and electricity generation from dewatered oily sludge in a bioelectrochemical system by rhamnolipid addition. Bioresour. Technol. 243, 820–827. https://doi.org/10.1016/j.biortech.2017.07.038.
Zhang, X., Zhang, N., Chen, Z., Ma, Y., Wang, L., Zhang, H., Jia, J., 2019. Long-term impact of sulfate on an autotrophic nitrogen removal system integrated partial nitrification, anammox and endogenous denitrification (PAED). Chemosphere 235, 336–343. https://doi.org/10.1016/j.chemosphere.2019.06.175.
Zhang, Z., Han, Y., Xu, C., Han, H., Zhong, D., Zheng, M., Ma, W., 2019. Effect of low-intensity direct current electric field on microbial nitrate removal in coal pyrolysis wastewater with low COD to nitrogen ratio. Bioresour. Technol. 287, 121465. https://doi.org/10.1016/j.biortech.2019.121465.
Zhao, F., Heidrich, E.S., Curtis, T.P., Dolfing, J., 2020. Understanding the complexity of wastewater: the combined impacts of carbohydrates and sulphate on the performance of bioelectrochemical systems. Water Res. 176, 115737. https://doi.org/10.1016/j.watres.2020.115737.
Zhu, T., Zhang, Y., Bu, G., Quan, X., Liu, Y., 2016. Producing nitrite from anodic ammonia oxidation to accelerate anammox in a bioelectrochemical system with a given anode potential. Chem. Eng. J. 291, 184–191. https://doi.org/10.1016/j.cej.2016.01.099.
Zhu, T., Zhang, Y., Liu, Y., Zhao, Z., 2021. Electrostimulation enhanced ammonium removal during fe (III) reduction coupled with anaerobic ammonium oxidation (Feammox) process. Sci. Total Environ. 751, 141703. https://doi.org/10.1016/j.scitotenv.2020.141703.